Automatica 90 (2018) 271–285

Contents lists available at ScienceDirect

Automatica

journal homepage: www.elsevier.com/locate/automatica

Image feedback based optimal control and the value of information in a differential game☆

Vladimir Macias [a], Israel Becerra [b], Rafael Murrieta-Cid [a,*], Hector M. Becerra [a], Seth Hutchinson [b]

[a] Centro de Investigación en Matemáticas, CIMAT, Guanajuato México, Mexico
[b] University of Illinois at Urbana-Champaign, Urbana, IL, USA

ARTICLE INFO

Article history:
Received 24 November 2016
Received in revised form 28 June 2017
Accepted 30 November 2017
Available online 15 February 2018

Keywords:
Pursuit/Evasion
Optimal control
Projective geometry
Feedback
Motion strategies

ABSTRACT

In this paper, we address pursuit-evasion problems in which the pursuer is a Differential Drive Robot (DDR) that attempts to capture an omnidirectional evader. From the Nash property it follows that if the evader deviates from its maximum potential speed then the capture time shall not increase for a pursuer that does not deviate from its Nash equilibrium motion strategy. However, it is not immediately clear how the pursuer could exploit that evader's deviation from its maximum potential speed, which might correspond to situations where the evader's capabilities may degrade with time, for example, battery depletion in an autonomous vehicle, or fatigue in an animal evader. This can be considered as a scenario of an evader in which the set of admissible controls varies with time. In the present paper we consider such scenario. In our first result, we propose an alternative strategy for the pursuer, which, for certain scenarios, further reduces the capture time compared to the strategy based on the maximum potential evader's speed. In our second result, we show that, under non-anticipative strategies, a pursuer strategy that uses the instantaneous evader speed alone, *does not always guarantee* to improve the payoff for the pursuer, nor the capture of the evader. Hence, we conclude that the evader's location is the relevant information for the pursuer to know. Later, we present vision-based control laws that implement the optimal pursuer strategy. The optimal pursuer strategy is characterized by a partition of the reduced space (a representation of the game in the pursuer's body-attached coordinate system) in which each region maps to an optimal pursuer action. We consider the case for which the pursuer is equipped with an omnidirectional catadioptric camera. Finally, in our third result we show that the location of the evader on the image can be directly used by the pursuer to define its motion strategy, in spite of the distortion of the state space suffered on the image. That is, the pursuer is able to apply its motion strategy using the image without explicitly reconstructing the evader's position. This approach is computationally efficient, and robust to occlusions and noise in the image.

1. Introduction

In this paper, we consider the pursuit-evasion problem of capturing an omnidirectional evader using a Differential Drive Robot (DDR) in an obstacle-free environment. More specifically, given an initial condition in which the evader is at distance L from the pursuer, the pursuer's goal is to reduce this distance to $L < l$ (the capture condition) as quickly as possible, while the evader's goal is to delay capture for as long as possible. The classical solution to this problem yields so-called Nash equilibrium strategies. While it is well known that neither player can improve its guaranteed payoff by unilaterally deviating from its Nash strategy, it is not always immediately clear how one player can exploit deviation from the Nash strategy by the other player. In this paper, we address this issue. We then present a vision-based control law that implements the optimal pursuer strategy (or policy).

The results in this paper are related to previous work presented in Jacobo, Ruiz, Murrieta-Cid, Becerra, and Marroquin (2015) and Ruiz, Murrieta-Cid, and Marroquin (2013). In Ruiz et al. (2013), the optimal strategies for each player are expressed in terms of a

☆ This work was partially funded by CONACYT projects 220796 and 264896, and post-doctoral fellowship 277028. The authors would also like to acknowledge the financial support of Intel Corporation for the development of this work. The material in this paper was partially presented at the IEEE International Conference on Robotics and Automation, May 26–May 30, 2015, Washington, USA. This paper was recommended for publication in revised form by Associate Editor C.C. Cheah under the direction of Editor Thomas Parisini.

* Corresponding author.
E-mail addresses: maciasandoval@cimat.mx (V. Macias), israelb4@illinois.edu (I. Becerra), murrieta@cimat.mx (R. Murrieta-Cid), hector.becerra@cimat.mx (H.M. Becerra), seth@illinois.edu (S. Hutchinson).

https://doi.org/10.1016/j.automatica.2017.12.045
0005-1098/

partition of the playing space into disjoint regions, and open-loop, time optimal strategies of the players are defined for each region. A feedback control strategy to implement the optimal pursuer strategy was presented in Jacobo et al. (2015). For this approach, computer vision-based state estimation was implemented using the 1D trifocal tensor (1D because only bearing information is used to compute it). The approach of Jacobo et al. (2015) was motivated by the possibility that an evader could avoid capture in cases where the pursuer executed its Nash strategy in open loop; nevertheless, Jacobo et al. (2015) did not address the issue of how the pursuer could exploit deviations by the evader from its maximum potential speed, which is addressed in this paper. Further, the approach of Jacobo et al. (2015) relied on position-based visual servo methods, which are known to be sensitive to state estimation errors or calibration inaccuracies (Chaumette & Hutchinson, 2006).

In this paper, we consider non-anticipative strategies (Elliott & Kalton, 1972) for both players (each player has complete up-to-date information concerning the control functions employed by the other player, however, it does not know the controls that the other player will apply in the future) and we investigate the scenario of an evader in which the set of admissible controls varies with the time. Namely, we consider an evader whose maximum speed varies as time elapses; to the best of our knowledge this problem has not been studied before in the context of differential games. We assume that the maximum potential speed of the evader V_e^{max} is known for the pursuer before the game commences. We consider $V_e(t)$ as the instantaneous maximum speed at which the evader can travel as time elapses, and V_e^{max} as the upper bound for that speed for all t. In Section 5 we investigate pursuer strategies exploiting deviations by the evader from its maximum potential speed and in Section 6 we present a vision-based control law that implements the optimal pursuer strategy. More precisely, in Section 5 we show that under a non-anticipative strategies framework, using the instantaneous evader speed *does not always guarantee* to improve the payoff for the pursuer, nor the capture of the evader, hence, the only information required for the pursuer is the evader's location. Based on this result, in Section 6, we show how to obtain this information, i.e., the evader's location directly in an image, without the estimation of the evader's state on the state space. Therefore, the connection between Section 5 and Section 6 consists in first proving that the evader's location is the relevant information for the pursuer and then, in order to retrieve the evader's location, we use the projection from the state space to the image space and we prove that under this projection, a partition of the state space defining the pursuer strategy can be mapped to the image space *in spite of* the distortion of the state space suffered on the image, allowing immediate determination of the optimal pursuer action once the evader is detected in the image. This approach is computationally efficient, and robust to occlusions and noise.

A preliminary version of a portion of Section 5 of the present work appeared in Becerra, Macias, and Murrieta-Cid (2015). The main results of the present work are the following:

- From the Nash property it follows that if the evader deviates from its maximum potential speed V_e^{max}, then the capture time shall not increase for a pursuer that follows a motion strategy generated by V_e^{max} (we refer to this pursuer strategy as $\Pi_{P(V_e^{max})}$). However, Theorem 1 proposes another strategy for the pursuer, called $\Pi_{P(V_e)}$, which, for certain scenarios, further reduces the capture time compared to $\Pi_{P(V_e^{max})}$.
- Theorem 2, which shows that under non-anticipative strategies, using instantaneously the partition obtained based on the instantaneous evader speed *does not always guarantee* to improve the payoff for the pursuer, nor the capture of the evader. In Lemma 2 (which is used in Theorem 2) we *exhibit* a case in which the evader escapes if the pursuer uses the strategy based on the instantaneous evader speed, that is strategy $\Pi_{P(V_e)}$. Therefore, under non-anticipative strategies, the evader's instantaneous speed cannot be used alone to improve the payoff and the pursuer must stick to the worst case corresponding to assuming that the evader moves at V_e^{max}.
- Finally, Theorem 3 shows that the location of the evader on the image can be directly used by the pursuer to define its motion strategy. That is, the pursuer is able to apply its motion strategy using the image without explicitly reconstructing the evader's position.

The remainder of this paper is organized as follows. In Section 2, we provide a review of related work. In Section 3, we give a formal description of the problem, and in Section 4 we describe the motion strategies for both pursuer and evader. In Section 5, we present the primary theoretical results in the paper, concerning the role of information in the optimality of Nash pursuer strategies when the evader moves at suboptimal speed. Finally, in Section 6, we derive image-based control strategies that implement the optimal pursuer strategy.

2. Related work

Our work is related to optimal control methods used in robotics, for instance Balkcom and Mason (2002), Soueres and Laumond (1996) and Wang, Chen, and Soueres (2009), however those methods typically execute the motion in open loop. Our work proposes a state feedback-based motion strategy, but using information directly from an image. Our work is also related to image-based visual servo (Chaumette & Hutchinson, 2006; Lopez-Nicolas, Gans, Bhattacharya, Sagues, & Hutchinson, 2010), in the sense that the feedback is directly based on an image, however, in contrast to the classical image-based visual servoing approach, in our proposed approach, the goal for the robot is not to see a target image, but instead its objective is to bring the evader to a specific locus of points called the *usable part* (Isaacs, 1965).

The problem addressed in this paper is a pursuit-evasion game. There has been a considerable amount of research in the area of pursuit and evasion, particularly in the area of control (Başar & Olsder, 1999; Isaacs, 1965; Merz, 1971). The pursuit-evasion problem can be framed as a problem in noncooperative dynamic game theory (Başar & Olsder, 1999).

A pursuit-evasion game can be defined in several ways. One variant considers one or more pursuers, which are given the task of *finding* an evader in an environment with obstacles (Guibas, Latombe, LaValle, Lin, & Motwani, 1999; Hollinger, Singh, Djugash, & Kehagias, 2009; Tovar & LaValle, 2008; Vidal, Shakernia, Jin, Hyunchul, & Sastry, 2002). A recent survey of this kind of problem is presented in Chung, Hollinger, and Isler (2011).

Other variant consists of *maintaining visibility of a moving evader* also in an environment with obstacles (Bandyopadhyay, Ang, & Hsu, 2007; Bhattacharya & Hutchinson, 2010; Jung & Sukhatme, 2002; LaValle, González-Baños, Becker, & Latombe, 1997; Murrieta-Cid, Muppirala, Sarmiento, Bhattacharya, & Hutchinson, 2007; O'Kane, 2008). Game theory is proposed in LaValle et al. (1997) as a framework to formulate the tracking problem, and an online algorithm is presented. In Bhattacharya and Hutchinson (2010), the authors address the problem of maintaining visibility of the evader as a *game of degree* (i.e. the emphasis is over the optimization of a given criterion and not over the problem of deciding what player is the winner). The pursuer and the evader are omnidirectional (holonomic) systems. In Bhattacharya and Hutchinson (2011), the problem of maintaining visibility of

a moving evader is addressed as a *game of kind* (deciding which player wins). Again, both the pursuer and the evader are omnidirectional systems. In Murrieta-Cid, Ruiz, Marroquin, Laumond, and Hutchinson (2011), the authors addressed the problem of tracking (maintaining surveillance) of an omnidirectional mobile evader at *constant* distance with a Differential Drive Robot in an environment without obstacles.

Similar to this work, in O'Kane (2008) the author deals with the information required to achieve the task. In that work, a robot has to track an unpredictable target. The robot's sensors obtain general information about the target's movements. An objective of O'Kane (2008) is to avoid the need for the agent to have detailed information about the target's movements, so that the agent does not allow damage to occur to the target. As in the present work, in O'Kane (2008) the author is also interested in the value of information, nevertheless, in O'Kane (2008) the information is addressed to preserve privacy, while in our work our interest in information is focused on obtaining optimality in the task given to the robot.

A third variant of pursuit-evasion problem consists in giving to the pursuer the goal *to capture the evader* (Isaacs, 1965; Merz, 1971), that is, move to a contact configuration, or closer than a given distance. The work presented in this paper corresponds to this third variant. Other related problems are the lady in the lake (Başar & Olsder, 1999) and the lion and the man (Flynn, 1974; Karnad & Isler, 2009). In the lady in the lake problem, there is a circular lake where a lady is swimming with a maximum speed v_l, and there is a man that is in the side of the lake and runs along the shore with a maximum speed v_m; the man cannot enter the lake and the lady wants to leave the lake. The man runs with a larger speed than the one of the lady in the lake ($v_l < v_m$). The man needs to capture the lady as soon as she reaches the shore, since on land she runs faster than him. In the lion and the man problem, the players move in a circular arena, both players have the same motion capabilities, the lion wants to capture the man and the man wants to avoid the capture.

In the same vein, in Isler and Karnad (2008) the authors address a pursuit-evasion game in a graph called the cops and robbers game. The cops win the game if they can move to the robber's vertex. Like the present work, the authors investigate the role of the available information, however, in Isler and Karnad (2008) the authors start from a base case where the players "see" each other at all times and then the authors reduce the visibility range of the players, while in the presented work, in Section 5, we start from Nash equilibrium strategies, make the players deviate from them, and start increasing the available information. Furthermore, in Isler and Karnad (2008) the authors are interested in the effects of information on the outcome of the game (which player wins), while we are interested in the deviations of the players over their time optimal strategies and the necessary information to detect such deviations to obtain optimality.

Section 6 of this work is related to ideas presented in LaValle (unpublished). In LaValle (unpublished), the author studies the preimages of sensors and provides a notion of dominant sensors. The sensors are hierarchically ordered by the information that they provide and the author suggests the use of combinatoric filters over the space and the time. Despite the similarities between this work and the one presented in LaValle (unpublished), there exists important differences. For instance, while in LaValle (unpublished) equivalent classes over the observations preimages (the state space) are used, in this work we propose to restrict the states and use directly the observations (that is, the images of the state space). Another important difference is that in LaValle (unpublished) functions are established between observations and states, while in this work we propose motion strategies that provide the robot controls.

3. System model

Each wheel of the DDR has associated a linear tangential velocity v but also a rotational angular velocity w. The relation between them is just $v = w \times r$, where r is the radius of the wheel. Thus, u_1 and u_2 are the wheels' angular velocities of the pursuer, more precisely, for the left wheel u_1 and the right wheel u_2. The linear velocity of the robot is $v = \frac{v_l+v_r}{2} = \frac{r(w_l+w_r)}{2}$, and its angular velocity is $\omega = \frac{v_r-v_l}{2b} = \frac{r}{2b}(w_r - w_l)$, being b the distance from the center of the robot to each wheel. In the paper r is assumed to be the same (1 for both wheels). With suitable choice of units and substituting that value of r, we obtain Eqs. (2). The absolute velocity (speed) of the evader is denoted by $v_1 \in [0, V_e^{\max}]$ and $v_2 \in [0, 2\pi)$ is the angle measured clockwise from the forward vector (heading) of the pursuer to the evader position in the reduced coordinate system. Eq. (1) is expressed in the form $\dot{\mathbf{x}} = f(\mathbf{x}, u, v)$, where $u = (u_1, u_2) \in U = [-V_p^{\max}, V_p^{\max}] \times [-V_p^{\max}, V_p^{\max}]$ and $v = (v_1, v_2) \in V = [0, V_e^{\max}] \times [0, 2\pi)$.

The model of the kinematics in the reduced coordinate system is the following.

$$\begin{aligned} \dot{x} &= \left(\frac{u_2 - u_1}{2b}\right) y + v_1 \sin v_2 \\ \dot{y} &= -\left(\frac{u_2 - u_1}{2b}\right) x - \left(\frac{u_1 + u_2}{2}\right) + v_1 \cos v_2 \end{aligned} \tag{1}$$

$$\begin{aligned} \omega &= \frac{u_2 - u_1}{2b} \\ v &= \frac{u_1 + u_2}{2} \\ |\omega^{\max}| &\leq \frac{1}{b}(V_p^{\max} - |v|). \end{aligned} \tag{2}$$

The inequality in the third line of Eqs. (2) (Balkcom & Mason, 2002; Murrieta-Cid et al., 2011) gives the maximum rate of rotation $\omega^{\max}$ for the pursuer, given a specified linear speed.

To simplify the problem, the game is modeled in a coordinate system that is fixed to the DDR (see Fig. 1(b)), called in Isaacs (1965) the *reduced space*. In the reduced space all the orientations are measured with respect to the positive y-axis (DDR's heading). We denote the state of the system as $\mathbf{x}(t) = (x, y) \in \mathbb{R}^2$.

The following definitions are used in the rest of the paper:

$$\rho_v = V_e^{\max}/V_p^{\max} \tag{3}$$

is the ratio between the maximum translational speed of both players, and

$$\rho_d = b/l \tag{4}$$

is the ratio of the distance between the center of the robot and the wheel location b and the capture distance l. Note that $l \geq b$, otherwise the capture distance would be located inside the robot.

4. Motion strategies

In this section, we present the motion strategies of both players. We begin presenting some basic concepts and definitions.

4.1. Basic concepts: strategies, payoff and the value function of the game

Let U and V be the control sets for each of the two players. Then, let $\mathcal{U}$ be the set of Lebesgue measurable maps $u : [t_s, \infty) \to U$, and $\mathcal{V}$ the set of Lebesgue measurable maps $v : [t_s, \infty) \to V$. The set $\mathcal{U}$ is the set of open loop strategies for the pursuer, and $\mathcal{V}$ the set of open loop strategies for the evader.

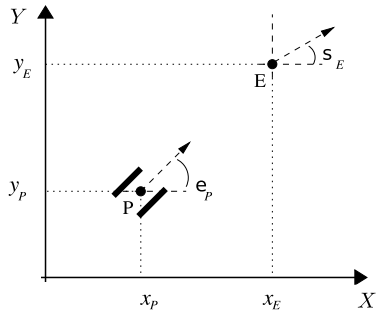

(a) Realistic space.

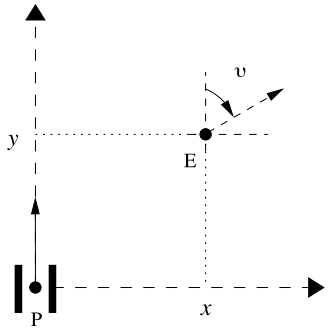

(b) Reduced space.

Fig. 1. System models.

Definition 1. The map $\alpha : \mathcal{V} \to \mathcal{U}$ is called a non-anticipative strategy if, whenever $t_s < T \leq t_f$ and $v_1(t) = v_2(t)$ a.e., $t_s \leq t \leq T$, then $\alpha(v_1)(t) = \alpha(v_2)(t)$ a.e., $t_s \leq t \leq T$ Elliott and Kalton (1972).

In the present game, the payoff J is represented by the capture time as shown in the equation below,

$$J(\mathbf{x}(t_s), u, v) = \int_{t_s}^{t_f(\mathbf{x}(t_s),u,v)} dt = t_f(\mathbf{x}(t_s), u, v) - t_s \tag{5}$$

where t_s is the starting time and t_f the ending time of the game. Indeed, if the evader wins, it is because the capture time is not finite, otherwise the pursuer wins.

Now, refer to $\mathcal{A}$ as the set of non-anticipative strategies for the pursuer, and denote the pursuer strategy as $\Pi \in \mathcal{A}$. Define equivalently for the evader the set $\mathcal{B}$, and its applied strategy as $\Gamma \in \mathcal{B}$. The upper value function $\boldsymbol{V}^+$ (Elliott & Kalton, 1972) is given by

$$\boldsymbol{V}^+ = \inf_{\Pi \in \mathcal{A}} \sup_{v \in \mathcal{V}} J(\mathbf{x}(t_s), \Pi(v), v). \tag{6}$$

Similarly the lower value function is

$$\boldsymbol{V}^- = \sup_{\Gamma \in \mathcal{B}} \inf_{u \in \mathcal{U}} J(\mathbf{x}(t_s), u, \Gamma(u)). \tag{7}$$

When $\boldsymbol{V}^+ = \boldsymbol{V}^-$ the game is said to have value.

The strategies of both players, the payoff and the value function of the game are all defined in the reduced space.

4.2. State space partition for motion strategies

In this section a partition of the state space into mutually disjoint regions is presented. This partition was found in Ruiz et al. (2013) using Isaacs' methodology (Isaacs, 1965), which combines the theory of optimal control and differential games. To make this paper self-contained, we include an Appendix with some lemmas and theorems obtained in Jacobo et al. (2015) and Ruiz et al. (2013), which are used in this work.

Fig. 2(a) shows a graphical representation of the regions that build the partition of the first quadrant of the reduced space. The frontiers between regions are called singular surfaces (Isaacs, 1965). In the present partition, there are 4 singular surfaces: universal surface (US, blue bold line), transition surface (TS, red curve), the barrier surface (BS, magenta straight line) and dispersal surface (DS, orange line). If the pursuer applies its time-optimal motion strategy the barrier (BS) cannot be crossed by the evader. The answer to the capture-escape question relies on whether or not the barrier divides the reduced space into two parts. Suppose the barrier separates it into two parts. If x is in the outer side then the DDR cannot force the capture. If the barrier fails to separate the playing space (as in Fig. 2(a)), then capture can be attained by the DDR.

Remark 1. If the barrier does not split the playing space for a given V_p^{max} and a given V_e^{max}, then the pursuer guarantees capture regardless of the strategy followed by the evader. See Theorem 4 in Appendix.

The universal surface (US), which is unbounded, has the property that whenever the evader is located at it, the time-optimal motion strategy for the pursuer is to move in a straight line to capture the evader. The limit of the US is at $y_c = l/\rho_v$ (see Fig. 2(a) and Lemma 5 in Appendix).

The transition surface (TS) is the place where a control variable abruptly changes its value. In contradistinction with the US and the BS, which correspond to trajectories of the system, the TS is not a trajectory traveled by the system in the reduced space. In the first quadrant, the TS represents the locus of points where the DDR switches one of its controls, in particular from Lemma 6 in Appendix, we found that u_2^* switches from the value $V_p^{\max}$ to $-V_p^{\max}$. The expression defining the control u_2^* at the moment of the switch characterizes the conditions that must be satisfied by the points (x, y) in the reduced space.

A dispersal surface (DS) is defined in Isaacs (1965) as the locus of initial conditions along which the optimal strategy of one or both players is not unique. At the DS, the choice of the control of one player must correspond to the choice of the control of the other player. Therefore, a solution will be to employ an instantaneous mixed strategy (Başar & Olsder, 1999), which means the randomizing of a player's decision in accordance with some probabilistic law until the system is no longer on the DS and this must be executed in closed loop.

The partition also contains the terminal surface and the usable part (UP). The terminal surface is the set of points that represents an opportunity for the DDR to capture the evader (Isaacs, 1965). In this game it is a circle of radius l. The usable part is an arc of a circle (UP, black bold arc in Fig. 2(a)), and is the portion of the space where the pursuer guarantees capture of the evader regardless of the choice of controls by the evader (Isaacs, 1965). The boundary of the usable part is the point BUP shown in Fig. 2(a). The angle s denotes the angle measured from the positive y-axis to a point in the usable part, and $S = \cos^{-1}(\rho_v)$ denotes a bound in s corresponding to the boundary of the usable part (BUP). See Fig. 2(b) and Lemma 7 in Appendix.

4.3. Pursuer motion strategy

In the interior of each region, the pursuer always applies its feedback-based time-optimal motion strategy obtained from the evader's location over the reduced space. This strategy for the first quadrant is summarized in Table 1 (which was obtained

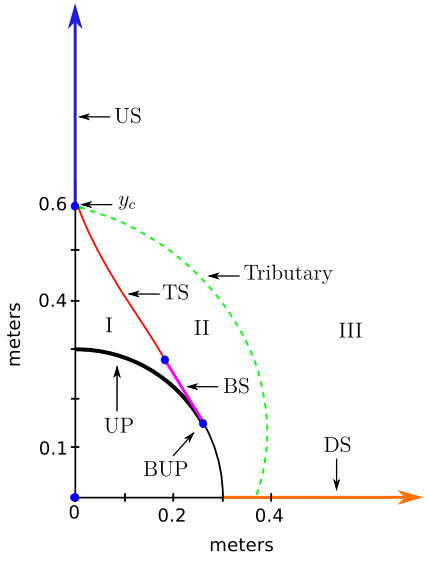

(a) Region I corresponds to straight line DDR motion and regions II and III to DDR rotation in place.

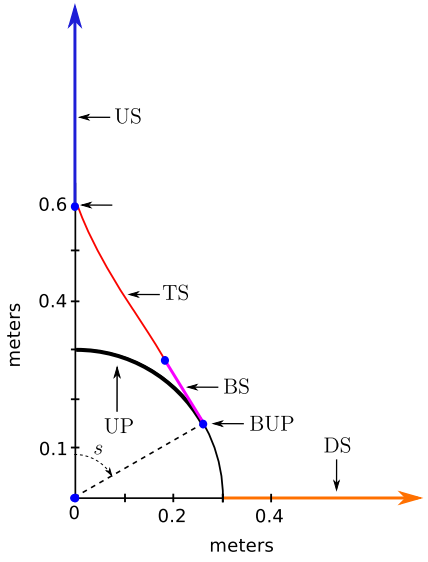

(b) Partition for pursuer's feedback motion strategy. Regions II and III are merged.

Fig. 2. Partition of the first quadrant. (For interpretation of the references to color in this figure legend, the reader is referred to the web version of this article.)

Table 1
Pursuer's feedback-based time-optimal motion strategy in quadrant 1.

Evader in the reduced space	u_1, u_2
US	$u_1 = +V_p^{\max}, u_2 = +V_p^{\max}$
I	$u_1 = +V_p^{\max}, u_2 = +V_p^{\max}$
II	$u_1 = +V_p^{\max}, u_2 = -V_p^{\max}$
III	$u_1 = +V_p^{\max}, u_2 = -V_p^{\max}$
DS	Randomized strategy

in state-based feedback form in Jacobo et al., 2015). In the remaining quadrants the pursuer time-optimal motion strategy is analogous.

If the evader is located in Region I then the DDR moves in a straight line in the realistic space to capture the evader. Region II corresponds to configurations in the realistic space where the DDR initially rotates in place, but it is not necessary to align completely the DDR's heading with the segment joining the positions of both players in order to capture the evader. Region III in the reduced space corresponds to configurations in the realistic space where the DDR also rotates in place until it aligns its heading with the segment joining the players' positions. The frontier between Region II and Region III is established by the tributary trajectory[1] (green dashed line) shown in Fig. 2(a).

From Table 1, we see that the US and Region I have associated the same optimal controls, and the same happens with regions II and III. Therefore, the partition shown in Fig. 2(a) might be simplified to one in which the US and Region I are merged and Region II and Region III are merged too. Hence, let $R_S = \text{US} \cup \text{Region I}$ and $R_R = \text{Region II} \cup \text{Region III}$. Refer to Fig. 2(b). The DS is not included in the set R_R. Over the DS, both players have two choices for their controls, to deal with this, a common approach is to use an instantaneous mixed strategy, for more details see Isaacs (1965).

4.4. Evader motion strategy

As mentioned above the pursuer motion strategy is determined by the partition of the reduced space. The regions are equivalence classes defined by the controls.

Note that in this game the pursuer wants to minimize the capture time and the evader wants to maximize it. Hence the pursuer is the minimizer and the evader the maximizer.

The evader controls that maximize the capture time associated to its motion strategy $\Gamma(t)$ were also obtained in Ruiz et al. (2013) using Isaacs' methodology (Isaacs, 1965). This methodology is an extension of the Pontryagin's Maximum Principle (PMP) (Pontryagin, Boltyanskii, Gamkrelidze, & Mishchenko, 1962) for two players. It is based on the computation of the Hamiltonian of the system and the so-called gradient of the value function $\nabla V = [V_x \;\; V_y]^T$ where V_x and V_y represent the partial derivatives $\frac{\partial V}{\partial x}$ and $\frac{\partial V}{\partial y}$. In the Isaacs' methodology a strategy (or policy) is in open loop. This means that it is based on retro-time and not on the position over the state space.

Differently to the pursuer, for the evader there are not equivalent classes grouping its controls, hence these controls and the associated evader motion strategy depend on every point in the reduced space (or equivalent for every given retro-time instant). The evader controls are v_1, its speed, and v_2, its motion direction or angle of motion. The optimal evader controls (Ruiz et al., 2013), those that maximize the capture time depend on the gradient of the value function and are given by:

$$v_1^* = V_e^{\max}, \;\; \sin v_2^* = \frac{V_x}{\rho}, \;\; \cos v_2^* = \frac{V_y}{\rho} \tag{8}$$

where $\rho = \sqrt{V_x^2 + V_y^2}$. The evader will also move at maximum speed. The resulting expressions for V_x and V_y are given in closed form in Ruiz et al. (2013) and they depend on the regions in the partition since, they consider both the optimal evader and pursuer motions. However, note that unlike the pursuer strategy, the evader optimal strategy is not piecewise constant in the reduced space.

5. Influence of the available information on the motion strategy

In this section, we investigate the scenario of an evader in which the set of admissible controls varies with the time. In particular, we consider an evader whose maximum speed varies as time elapses and the effects of this deviation over the pursuer strategy. Recall

[1] A tributary trajectory is an optimal trajectory of the system in the reduced space that reaches the US.

that we assume that the maximum potential speed of the evader V_e^{max} is known for the pursuer before the game commences. We consider $V_e(t)$ as the instantaneous maximum speed at which the evader can travel as time elapses, and V_e^{max} as the upper bound for that speed for all t. Since $V_e(t)$ is assumed to be the evader's current maximum speed capacity, we consider its variation as a change in the evader's control set, that is, $v = (v_1, v_2) \in [0, V_e(t)] \times [0, 2\pi)$, rather than a cooperation from the evader.

As mentioned in Remark 1, if the barrier does not split the playing space for a given V_p^{max} and a given V_e^{max}, then there exists at least a pursuer strategy that guarantees capture regardless of the strategy followed by the evader (Ruiz et al., 2013). In the remainder of the paper, it is assumed that the barrier will not split the reduced space.

Consider the DDR in the reduced space as the disk $D(\mathbf{0}; l)$ with the center at the origin and radius l, and let $\mathcal{C}$ be the collection of all the partitions of $\mathbb{R}^2 - D(\mathbf{0}; l)$. Then consider the function $P : \mathbb{R}_{>0} \to \mathcal{C}$ such that P maps the evader's maximum instantaneous speed V_e to a partition $P(V_e)$ as defined in Section 4.3. In the first quadrant of the reduced space, this partition has as elements regions R_S and R_R.

Partition $P(V_e)$ yields a motion strategy for the pursuer according to Table 1. Recall that the pursuer's strategy is denoted by Π, and Γ denotes the motion strategy of the evader. In this section we will consider the non-anticipative strategies $\Pi_{P(V_e)}$ and $\Gamma_{P(V_e)}$, where $\Pi_{P(V_e)} : \mathbb{R}^2 \times [0, V_e^{\max}] \to \mathcal{U}$, denotes the purser's strategy that applies the controls according to partition $P(V_e)$, and analogously $\Gamma_{P(V_e)} : \mathbb{R}^2 \times [0, V_e^{\max}] \to \mathcal{V}$ for the evader. The evader motion direction is obtained as described in Section 4.4 and v_1 is set to $V_e(t)$. Particularly, $\Pi_{P(V_e^{\max})} : \mathbb{R}^2 \to \mathcal{U}$ is the state feedback strategy proposed in Jacobo et al. (2015), which considers a fixed partition $P(V_e^{\max})$ during all the game since the upper bound $V_e^{\max}$ remains fixed for all t. Notice that $\Pi_{P(V_e^{\max})}$ can be interpreted as a non-anticipative strategy, considering a mapping from $\mathcal{V}$ to the space of state trajectories via Eq. (1), and then from the state trajectory to $\mathcal{U}$, via the state feedback control law. Moreover, if the evader does move with $V_e^{\max}$, both $\Pi_{P(V_e^{\max})}$ and $\Pi_{P(V_e)}$ coincide and yield the same pursuer behavior. Similarly, $\Gamma_{P(V_e^{\max})} : [t_s, \infty) \to V$, which is the open loop strategy in Nash equilibrium given in Ruiz et al. (2013), also considers a fixed partition.

Let us start with Lemma 1 saying that for any two partitions $P(V_e)$ and $P(V_e')$ with $V_e' < V_e$, then $R_S \in P(V_e)$ is fully contained in $R_S' \in P(V_e')$.

Lemma 1. *Let V_e and V_e' be speeds with $V_e' < V_e$, and $P(V_e)$ and $P(V_e')$ the respective partitions of the reduced space. Then, $R_S \subset R_S'$ where $R_S \in P(V_e)$ and $R_S' \in P(V_e')$.*

Proof. Let us consider the first quadrant. The rest of the quadrants are analogous cases due to the symmetry of the partitions. Regions $R_S \backslash \text{US} \in P(V_e)$ and $R_S' \backslash \text{US}' \in P(V_e')$ are bounded, and are respectively delimited by UP ∪ BS ∪ TS ∪ Y, and UP′ ∪ BS′ ∪ TS′ ∪ Y′, where Y and Y′ are the line segments delimited by UP and the points y_c and y_c', respectively. The main idea is to prove that UP ⊂ UP′, Y ⊂ Y′ and TS ∪ BS ⊂ R_S'.

(a) The angles $S = \cos^{-1}(\rho_v)$ and $S' = \cos^{-1}(\rho_v')$ delimit the usable parts UP and UP′, respectively (see Lemma 7 in Appendix and Fig. 3(a)). Given that $V_e' < V_e$, then $\rho_v' < \rho_v$. Additionally, $\cos S' < \cos S$, which as we are in the first quadrant, implies that $S < S'$. Therefore UP ⊂ UP′.

(b) The points y_c and y_c' are defined as $y_c = l\frac{V_p^{max}}{V_e}$ and $y_c' = l\frac{V_p^{max}}{V_e'}$ (see Lemma 5 in Appendix). Given that $V_e' < V_e$, it follows that $y_c < y_c'$. Hence, Y ⊂ Y′.

(c) The coordinates of TS and TS′ are given by

$$x(s) = l\sin s - b\rho_v \cos s;$$
$$y(s) = b\cot s + l\cos s - b\rho_v \frac{\cos^2 s}{\sin s} \tag{9}$$

$$x'(s) = l\sin s - b\rho_v' \cos s;$$
$$y'(s) = b\cot s + l\cos s - b\rho_v' \frac{\cos^2 s}{\sin s}. \tag{10}$$

Eqs. (9) and (10) were obtained in Jacobo et al. (2015), please see that work for more details.

Let us consider the next angles according to Lemmas 8 and 9 in Appendix:

$$s_c' = \tan^{-1}\left(\rho_d \rho_v'\right), \quad s_c = \tan^{-1}\left(\rho_d \rho_v\right),$$
$$S = \cos^{-1}\left(\rho_v\right) \quad \text{and} \quad S' = \cos^{-1}\left(\rho_v'\right).$$

Then, we have the next intervals: (see Fig. 3(b))

$$\left[0, s_c'\right], \left(s_c', s_c\right], \quad (s_c, S], \quad \text{and} \quad \left(S, S'\right].$$

(i) Let $s \in \left[0, s_c'\right]$. For TS, the optimal trajectory for angle s reaches the y-axis at point y_c starting from the UP in retro-time ($\tau = t_f - t$) (Isaacs, 1965). In a similar manner, for TS′ the optimal trajectory for an angle s reaches the y-axis at point y_c'. Given that $y_c < y_c'$, it follows that for such s, the TS is below TS′, therefore TS is contained in R_S'.

(ii) Let $s \in \left(s_c', s_c\right]$. Considering TS, the optimal trajectory in retro-time for an angle s starting from UP, reaches the y-axis at point y_c, in time $\tau_c < \tau_s$, where τ_s is the time at which the DDR switches controls. If we extend this trajectory beyond y_c, then we have $y_c < y(s)$. Given that $\rho_v' < \rho_v$ by Eqs. (9) and (10), we have that $y(s) < y'(s)$. Then $y_c < y'(s)$. Hence, in the interval $\left(s_c', s_c\right]$ the TS is below TS′.

(iii) Let $s \in (s_c, S]$. Given that $\rho_v' < \rho_v$, by Eqs. (9) and (10) we have that $x(s) < x'(s)$ and $y(s) < y'(s)$, which implies that in the interval $s \in (s_c, S]$, TS is below TS′.

(iv) Let $s \in \left(S, S'\right]$. Given that the UP is delimited by angle S, the trajectory with angle s does not end (in retro-time) in the TS.

Therefore the TS ⊂ R_S'

(d) The BS is a line segment that starts (in retro-time) in the frontier of the usable part (BUP) and ends at point $(x(S), y(S))$, which results from evaluating Eqs. (9) at angle S. Similarly, the BS′ starts at BUP′ and it ends at $(x'(S), y'(S))$. Given that $S < S'$ and using Eqs. (9), it follows that the BS ⊂ R_S'. ■

Remark 2. If $V_e' < V_e$ and $P(V_e')$, $P(V_e)$ are their corresponding partitions, then the first quadrant of the reduced space is divided in three regions: R_S, $R_S' - R_S$ and R_R' (see Fig. 4). The region $R_S' - R_S$ contains those points at which the pursuer control strategy is different for V_e' versus V_e.

Next, we present our first result Theorem 1, which is a result about existence. Nash equilibrium does not elaborate on the existence of a new strategy that improves the payoff for a player that takes advantage of the deviation of the other player from its optimal strategy; neither does it tell which extra information is needed in order to apply the new strategy if it exists. Following this line, through Theorem 1 we show that when the evader deviates from its maximum potential speed, there exist cases in which the pursuer can further reduce the capture time when it uses the instantaneous partition.

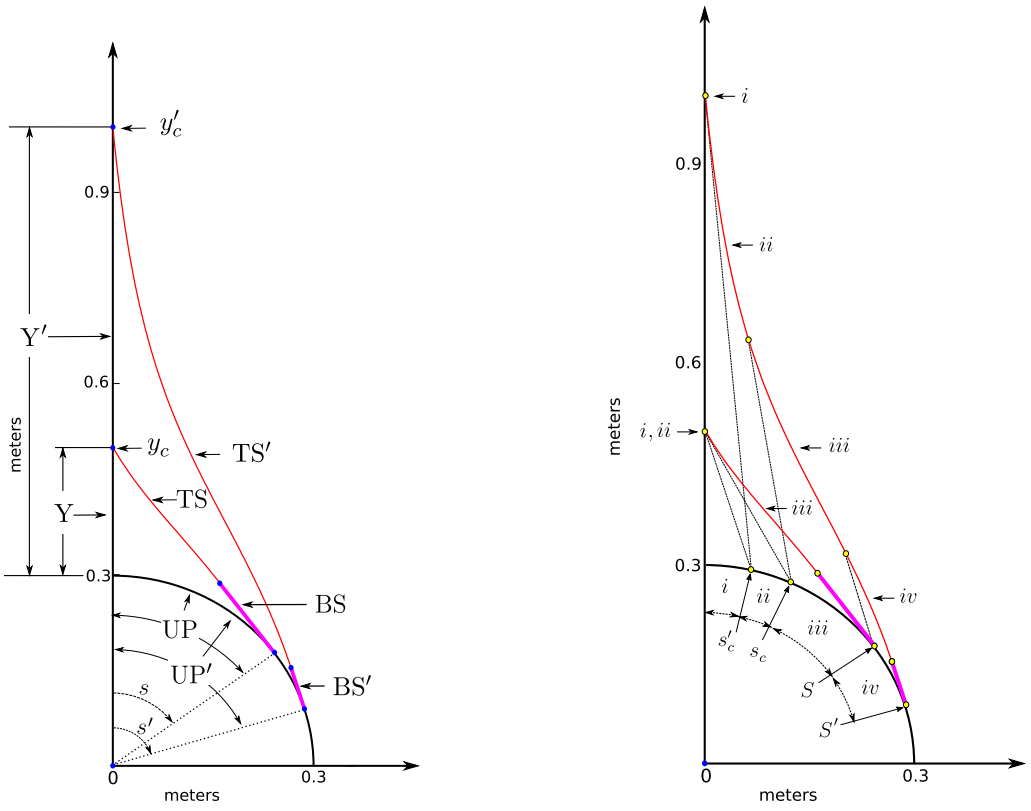

(a) Partition P and P'.

(b) Angular sectors defined in the proof of Lemma 1.

Fig. 3. Partitions P and P', and s angle intervals.

From the Nash property, if the evader deviates from its maximum potential speed V_e^{max} then the capture time shall not increase for a pursuer that follows the partition generated by V_e^{max} (the corresponding pursuer strategy is called $\Pi_{P(V_e^{max})}$, and it was obtained in Ruiz et al., 2013), that is: $J(x(t_s), \Pi_{P(V_e^{max})}, \Gamma_{P(V_e)}) \leq J(x(t_s), \Pi_{P(V_e^{max})}, \Gamma_{P(V_e^{max})})$. However, in Theorem 1, another strategy for the pursuer is proposed, namely, strategy $\Pi_{P(V_e)}$, which under certain scenarios, further reduces the capture time compared with $\Pi_{P(V_e^{max})}$, that is: $J(x(t_s), \Pi_{P(V_e)}, \Gamma_{P(V_e)}) < J(x(t_s), \Pi_{P(V_e^{max})}, \Gamma_{P(V_e)}) \leq J(x(t_s), \Pi_{P(V_e^{max})}, \Gamma_{P(V_e^{max})})$.

Theorem 1. *There exist scenarios where*
$J(\mathbf{x}(t_s), \Pi_{P(V_e)}, \Gamma_{P(V_e)}) < J(\mathbf{x}(t_s), \Pi_{P(V_e^{max})}, \Gamma_{P(V_e)})$.

Proof. We present a concrete scenario where strategy $\Pi_{P(V_e)}$ yields a smaller capture time than strategy $\Pi_{P(V_e^{max})}$. Let us consider $l = 1$, $b = 0.75$, $V_p^{max} = 1$, $V_e^{max} = 0.6$, and $q_1 = (0.8363, 0.6261)$, where l is the DDR radius, b is the distance between the DDR center and its wheels, and q_1 is the initial location of the system in the reduced space. Assume that the evader moves with constant speed $V_e = 0.3$. Now, construct partitions $P(V_e^{max})$ and $P(V_e)$ corresponding to V_e^{max} and V_e respectively. Under these conditions, while the DDR manages to capture the evader applying strategy $\Pi_{P(V_e)}$, strategy $\Pi_{P(V_e^{max})}$ does not manage to capture the evader in the same time interval. In Fig. 5 it can be seen that in the same time interval, applying strategy $\Pi_{P(V_e)}$ the DDR captures the evader (cyan trajectory) while with strategy $\Pi_{P(V_e^{max})}$ it still does not (blue trajectory). ■

Corollary 1. *There exist innumerably many scenarios such that strategy $\Pi_{P(V_e)}$ yields a smaller capture time than the capture time obtained while applying $\Pi_{P(V_e^{max})}$.*

Proof. A whole set Ω of such scenarios can be built in the next manner. Assume that the evader will be moving with a speed $V_e(t) < V_e^{max}$, and that $P(V_e^{max}) = \{R_S, R_R\}$ and $P(V_e) = \{R'_S, R'_R\}$. Consider Ω as the set of scenarios such that when the pursuer applies $\Pi_{P(V_e)}$, then $\mathbf{x}(t)$ is located in $R'_S \setminus R_S$, $\forall t \in [t_s, t_f)$, and such that $t_f(\mathbf{x}(t_s), \Pi_{P(V_e)}, \Gamma_{P(V_e)}) < t_f(\mathbf{x}(t_s), \Pi_{P(V_e^{max})}, \Gamma_{P(V_e)})$. A subset of Ω corresponds to scenarios where the system initial state $\mathbf{x}(t_s)$ is located in $R'_S \setminus R_S$ and $V_e(t)$ is constant. ■

Now we consider the particular case in which the evader moves with a constant speed during all the play. More specifically, in Propositions 1 and 2 we assume that the current control of the evader, v_1, corresponds to a constant speed $V_e < V_e^{max}$, however, strategy $\Pi_{P(V_e)}$ is the same non-anticipative strategy referred above, hence, it still does not know the future actions of the evader, that is, the pursuer does not know that the evader's speed will remain constant. Proposition 1 states that for that special case when the evader moves to constant speed V_e, the pursuer strategy $\Pi_{P(V_e)}$ is optimal, i.e. the one that reduces the most the capture time, namely: $V(\mathbf{x}(t_s)) = J(\mathbf{x}(t_s), \Pi_{P(V_e)}, \Gamma_{P(V_e)})$. On the other hand, Proposition 2 is a particular case of Theorem 1 in which the evader moves at constant speed, and states that for this specific setting, even under non-anticipative strategies, it is guaranteed that by using the instantaneous partition the pursuer cannot perform worse than using the partition generated by V_e^{max}.

Proposition 1. *If the evader moves at all time at a constant speed V_e, with $0 < V_e < V_e^{max}$, then $\boldsymbol{V}(\mathbf{x}(t_s)) = J(\mathbf{x}(t_s), \Pi_{P(V_e)}, \Gamma_{P(V_e)})$.*

Proof. The motion strategy in Nash-equilibrium $\Pi_{P(V_e^{max})}$, considers that the evader will move using the boundary speed of its capabilities, that is V_e^{max}. An evader e that moves with a constant speed V_e during all the play is equivalent to an evader e' with

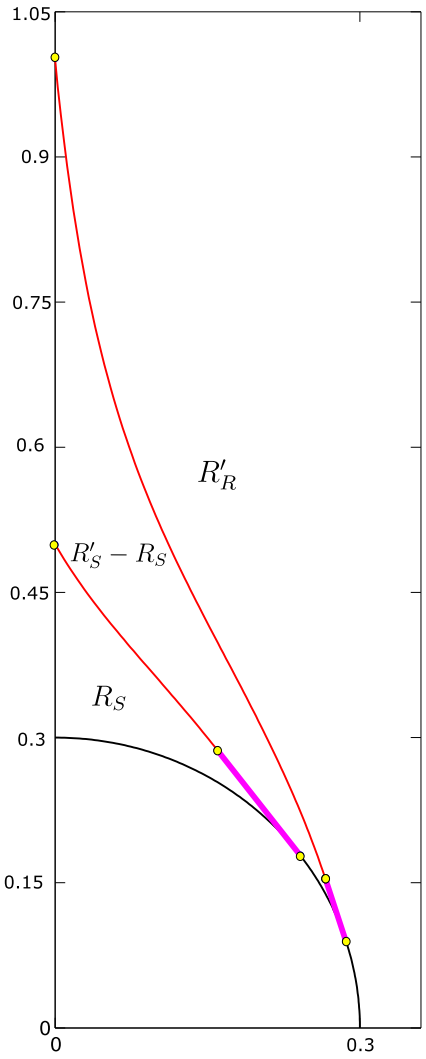

Fig. 4. Region $R'_S - R_S$.

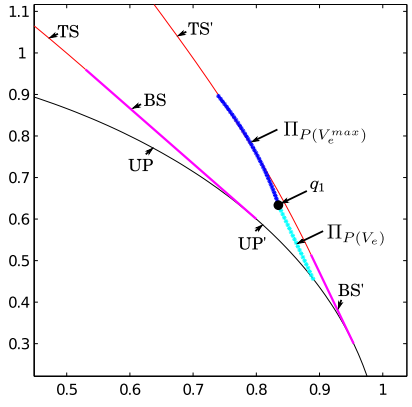

Fig. 5. Example of Theorem 1. (For interpretation of the references to color in this figure legend, the reader is referred to the web version of this article.)

$V_e'^{max} = V_e$, that is to move at the new boundary speed of its capabilities. Therefore, the corresponding optimal motion strategy for the DDR to play against e' is to apply the controls dictated by partition $P(V_e)$, which is what strategy $\Pi_{P(V_e)}$ exactly does. For the evader, the optimal controls are given by Eq. (8) considering $V_e'^{max} = V_e$ (maximum available speed), yielding strategy $\Gamma_{P(V_e)}$, which depends on the partition $P(V_e)$). Therefore $J(\mathbf{x}(t_s), \Pi_{P(V_e)}, \Gamma_{P(V_e)})$ is the value of the game $\boldsymbol{V}(\mathbf{x}(t_s))$. The result follows. ■

Furthermore, $\Pi_{P(V_e)}$ yields a smaller or equal capture time than $\Pi_{P(V_e^{max})}$, which is proven in the following proposition.

Proposition 2. *If the evader moves at all time at a constant speed V_e, with $0 < V_e < V_e^{max}$, then $J(\mathbf{x}(t_s), \Pi_{P(V_e)}, \Gamma_{P(V_e)}) \leq J(\mathbf{x}(t_s), \Pi_{P(V_e^{max})}, \Gamma_{P(V_e)})$.*

Proof. Strategy $\Pi_{P(V_e^{max})}$ for the pursuer, and strategy $\Gamma_{P(V_e^{max})}$ for the evader (considering that it travels with speed V_e^{max}) are the Nash-equilibrium strategies for this game (Ruiz et al., 2013), meaning that any unilateral deviation of a player from the optimal strategies does not provide it a benefit in its payoff J. In this game the payoff is the capture time, so if the evader deviates from speed V_e^{max} while the DDR continues applying $\Pi_{P(V_e^{max})}$, the evader can only perform worse, but not better. Furthermore, by Proposition 1, under the referred scenario, $\Pi_{P(V_e)}$ gives the optimal strategy for the DDR, and the optimal strategy for the evader is $\Gamma_{P(V_e)}$ with $V_e'^{max} = V_e$. Both strategies $\Pi_{P(V_e)}$ and $\Pi_{P(V_e^{max})}$ can deliver only two possible controls, either move in a straight line or rotation in place. Refer to Fig. 3(a). When the two disagree in the delivered control, the one yielding the smaller payoff is $\Pi_{P(V_e)}$ because it delivers the optimal control as stated in Proposition 1. When the controls agree the payoff may be smaller or equal depending on the initial location of the evader. Under this last scenario two cases might arise: one, that the evader directly reaches the UP, and two, that strategy $\Pi_{P(V_e)}$ requires a switch on the optimal control before $\Pi_{P(V_e^{max})}$ does. In the first case, the time is equal for both $\Pi_{P(V_e)}$ and $\Pi_{P(V_e^{max})}$, and in the second case the time to capture is smaller for $\Pi_{P(V_e)}$ than for $\Pi_{P(V_e^{max})}$. Hence, $J(\mathbf{x}(t_s), \Pi_{P(V_e)}, \Gamma_{P(V_e)}) \leq J(\mathbf{x}(t_s), \Pi_{P(V_e^{max})}, \Gamma_{P(V_e)})$. ■

Nonetheless, there are also cases in which despite the inclusion of more precise information, namely the instantaneous evader speed $V_e(t)$, the pursuer cannot improve its payoff J, as it must apply the worst case strategy $\Pi_{P(V_e^{max})}$, otherwise the capture of the evader is no longer guaranteed. Lemma 2 presents a family of pathological examples, such that when the pursuer at time t *instantaneously* applies the controls dictated by $\Pi_{P(V_e)}$, then the evader capture is not guaranteed even when the conditions mentioned in Remark 1 are met, meaning that, the capture is possible applying the strategy $\Pi_{P(V_e^{max})}$. Making use of Lemma 2 and other arguments, we introduce Theorem 2, which says that under a non-anticipative strategies framework, a pursuer strategy that uses the instantaneous evader speed by itself, does not guarantee to improve the payoff for the pursuer, nor the capture of the evader.

Lemma 2. *There exist scenarios where strategy $\Pi_{P(V_e)}$ makes the system indefinitely move in a cycle in the reduced space, avoiding the system to ever reach the UP.*

Proof. In Fig. 6 we present a concrete scenario where this happens. Assume that the evader's speed will take two possible values, V_e^{max} and V_e, for some fixed V_e, with $0 < V_e < V_e^{max}$. Let $P(V_e^{max}) = \{R_S, R_R\}$ and $P(V_e) = \{R'_S, R'_R\}$ be the corresponding partitions to such speeds, respectively. Also assume, that the barrier does not close. Let $q_1 \in R'_S \setminus R_S$ be the starting point of the play, and let us consider that the evader will start moving with speed V_e^{max}. Then, the DDR must apply the controls given by strategy $\Pi_{P(V_e^{max})}$ while the evader applies strategy $\Gamma_{P(V_e^{max})}$, namely, the DDR must rotate on site, hence, the system follows trajectory $C2$. When the system is at q_2, the evader changes its speed to V_e and applies strategy $\Gamma_{P(V_e)}$. Therefore, the DDR applies the controls given by

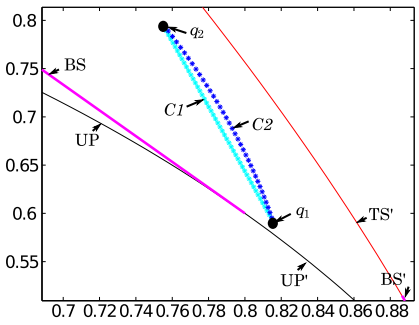

Fig. 6. Example of Lemma 2.

strategy $\Pi_{P(V_e)}$, that is, the DDR moves in a straight line motion with maximum speed. Then, the system follows trajectory $C1$, until it reaches again q_1. If this situation continues indefinitely, then the evader avoids capture whether or not the barriers in $P(V_e^{max})$ and $P(V_e)$ are closed. ■

Note that Lemma 2 does not contradict Theorem 1. Theorem 1 and Lemma 2 are results about existence. There exist cases in which when the pursuer uses the instantaneous partition, that is $\Pi_{P(V_e)}$, the pursuer can reduce the capture time, compared with the Nash Equilibrium strategy –Theorem 1 –, but there are also cases in which the pursuer cannot reduce the capture time and even worse, the evader escapes — Lemma 2.

Theorem 2. *Consider that the pursuer has only access to the evader's instantaneous maximum speed $V_e(t)$ (for the current t) and its upper bound V_e^{max}, further, the pursuer does not know $V_e(\mathrm{T})$ for $\mathrm{T} > t$. Then, using the instantaneous maximum speed $V_e(t)$ alone, does not guarantee to further reduce $J(\mathbf{x}(t_s), \Pi_{P(V_e^{max})}, \Gamma_{P(V_e)})$, nor the capture of the evader.*

Proof. Let us assume that the evader is traveling at a speed $V_e < V_e^{max}$ applying strategy $\Gamma_{P(V_e)}$. Since the only information available to the pursuer is the evader's instantaneous speed $V_e(t)$ and its upper bound V_e^{max}, then using the Isaacs methodology it is only possible to compute the instantaneous state space partitions yielding the instantaneous pursuer strategy $\Pi_{P(V_e)}$, or to compute $\Pi_{P(V_e^{max})}$. Next, we proceed to give sets of evader's positions where applying $\Pi_{P(V_e)}$ does not improve the payoff $J(\mathbf{x}(t_s), \Pi_{P(V_e^{max})}, \Gamma_{P(V_e)})$ for a pursuer that applies $\Pi_{P(V_e^{max})}$.

Consider $P(V_e^{max}) = \{R_S, R_R\}$ and $P(V_e) = \{R'_S, R'_R\}$. By Lemma 1, in partition $P(V_e^{max})$ region R_S is delimited by any other region $R'_S \in P(V_e)$. If over the reduced space the evader is within region R_S, strategies $\Pi_{P(V_e^{max})}$ and (any) $\Pi_{P(V_e)}$ dictate the same pursuer's control, hence, the pursuer achieves capture in both partitions traveling in a straight line. Therefore for a pursuer that applies $\Pi_{P(V_e^{max})}$ there is no use in considering the instantaneous speed V_e to reduce $J(\mathbf{x}(t_s), \Pi_{P(V_e^{max})}, \Gamma_{P(V_e)})$.

If the evader is within $R'_S \setminus R_S$, $\Pi_{P(V_e^{max})}$ dictates the pursuer to travel in a straight line, and $\Pi_{P(V_e)}$ that the pursuer rotates on site. In $R'_S \setminus R_S$ is the place where the pathological example described in Lemma 2 exists, and the pursuer does not know if the evader will be changing between speeds $V_e(t)$ and V_e^{max}. This indicates that in $R'_S \setminus R_S$ the pursuer must opt for strategy $\Pi_{P(V_e^{max})}$, as such strategy achieves capture for each evader's speed V_e bounded by V_e^{max} (Remark 1), and considers the most restrictive partition (the partition with the smallest UP, Lemma 1) as it is the only one that guarantees capture of the evader in the worst case (evader traveling at V_e^{max}) when it is outside region R_S. Thus, in $R'_S \setminus R_S$ the pursuer must not use strategy $\Pi_{P(V_e)}$ and apply strategy $\Pi_{P(V_e^{max})}$, that is, using the current instantaneous speed V_e cannot reduce $J(\mathbf{x}(t_s), \Pi_{P(V_e^{max})}, \Gamma_{P(V_e)})$, nor guarantee the evader's capture.

If the evader is in R'_R, the controls for the pursuer given by strategies $\Pi_{P(V_e)}$ and $\Pi_{P(V_e^{max})}$, are the same, which make the pursuer to rotate on site. As a consequence the instantaneous evader's speed V_e is not useful to reduce $J(\mathbf{x}(t_s), \Pi_{P(V_e^{max})}, \Gamma_{P(V_e)})$. If the pursuer keeps rotating on site it eventually takes the system to $R'_S \setminus R_S$, which takes us to region $R'_S \setminus R_S$ analyzed above, or to the universal surfaces where the strategies agree that the pursuer must travel on a straight line, hence the evader's speed V_e can be discarded.

The past analysis is exhaustive in the possible regions where the evader might be, hence the evader's instantaneous speed $V_e(t)$ by itself cannot be used to improve $J(\mathbf{x}(t_s), \Pi_{P(V_e^{max})}, \Gamma_{P(V_e)})$. Note, that the same analysis can be applied for any $V_e < V_e^{max}$. The result follows. ■

Theorem 2 is an exhaustive analysis of all the possible regions where the evader might be. We proved that in some regions, the capture time cannot be further reduced by applying $\Pi_{P(V_e)}$ against applying $\Pi_{P(V_e^{max})}$, so $\Pi_{P(V_e^{max})}$ is selected. In other regions, regions where the scenarios given in Theorem 1 might take place (scenarios where $\Pi_{P(V_e)}$ does improve the capture time), the possible improvement yielded by $\Pi_{P(V_e)}$ is overshadowed by the possibility that the pathological scenarios in Lemma 2 might happen, hence, strategy $\Pi_{P(V_e^{max})}$ must be applied in order to guarantee capture. Because strategy $\Pi_{P(V_e)}$ is non-anticipative and therefore it cannot foresee the evader's behavior, it is unable to discern if the actual play corresponds to a scenario like the one in Theorem 1 or the one in Lemma 2, so $\Pi_{P(V_e^{max})}$ is used instead. In conclusion, in every region $\Pi_{P(V_e^{max})}$ must be used instead of $\Pi_{P(V_e)}$, and strategy $\Pi_{P(V_e)}$, despite of using more precise information (evader's current maximum speed), cannot be used due to its non-anticipative nature; this shows that an increment in information does not always translate into a gain in the game payoff. Further, the only information required for the pursuer is the evader's location. In the section below, we show how to obtain the evader's location directly from an image, without its estimation on the state space.

Although knowing the instantaneous evader speed *does not always guarantee* the capture of the evader under non-anticipative strategies, the case of anticipative strategies opens a research subject, in which the optimal strategies may be different from $\Pi_{P(V_e^{max})}$ for the pursuer and $\Gamma_{P(V_e^{max})}$ for the evader. The guarantees presented in Propositions 1 and 2, which consider an evader's constant speed scenario, were attainable since the non-anticipative strategy $\Pi_{P(V_e)}$ is able to consider the actual value of the evader's maximal speed $V_e(t)$, and $V_e(t)$ remains constant, then $\Pi_{P(V_e)}$ is equivalent to applying an *anticipative* strategy. It remains to be investigated how to generally extend the Isaacs' methodology (Isaacs, 1965) to anticipative strategies when the players' controls change with time, which by Propositions 1 and 2 looks promising. We propose it as future work.

6. Motion strategy based on the image space with an omnidirectional camera

In this section, we will assume that the DDR is equipped with an omnidirectional camera. Next, we will provide a feedback motion strategy for the DDR pursuer that uses the evader's location directly from images taken by the camera.

6.1. Generic model for omnidirectional cameras

A vision system is called central when the sensed rays of light are intersected in a single point, called the center of projection. Some examples of a central vision system are: (1) Perspective cameras also called pinhole (they are conventional cameras), (2) some

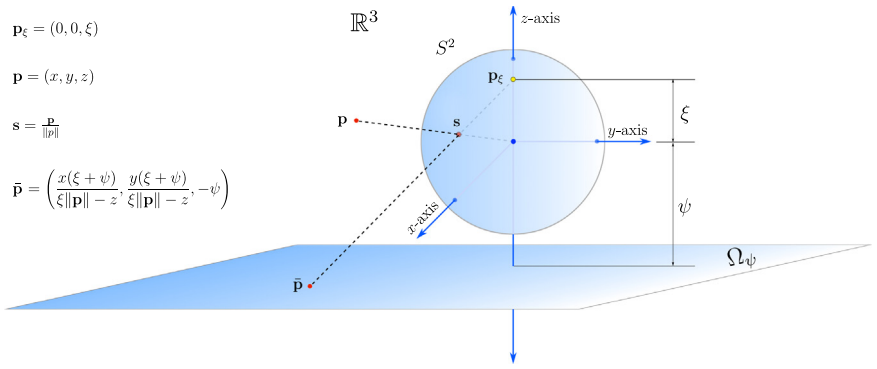

Fig. 7. Scheme of the generic model of a central camera.

Fish-eye cameras (the field of view of this system is larger than the one in perspective cameras) and (3) Omnidirectional catadioptric cameras or central catadioptric systems; these systems are based on light reflection and the use of curved mirrors (the field of view of this system is 360°). In the central catadioptric systems, the mirrors play an important role. The shape of the mirror determines the projection of a point in the space over the image plane. The mirror can be of different types. The more common are the parabolic and hyperbolic ones. In this subsection, we will apply the generic model of projection proposed in Geyer and Daniilidis (2000).

Let us consider the set $(\mathbb{R}^3)^* = \mathbb{R}^3 - \{(0,0,0)\}$, the unit sphere centered on the origin $S^2 = \{(x,y,z) \in (\mathbb{R}^3)^* : \|(x,y,z)\| = 1\}$ and the image plane $\Omega_\psi := \{(x,y,z) \in \mathbb{R}^3 : z = -\psi\}$. Over the plane Ω_ψ we project points of $\mathbb{R}^3$ (see Fig. 7). Let us first define $\pi_{S^2} : (\mathbb{R}^3)^* \to S^2$ by $\pi_{S^2}(\mathbf{p}) = \frac{\mathbf{p}}{\|\mathbf{p}\|}$. Then π_{S^2} projects each point $\mathbf{p} \in (\mathbb{R}^3)^*$ onto the sphere S^2.

On the other hand, let us select a point $\mathbf{p}_\xi = (0,0,\xi)$ with $\xi \in [0,1]$. Let $S_\xi := \{(x',y',z') \in S^2 : -1 < z' < \xi\}$. For each $\mathbf{s} = (x',y',z') \in S_\xi$ consider the ray that passes from the point $\mathbf{p}_\xi$ through $\mathbf{s}$. This ray intersects to Ω_ψ at a single point. Thus, this defines a function $\pi_{\Omega_\psi} : S_\xi \to \Omega_\psi$ given by $\pi_{\Omega_\psi}(\mathbf{s}) = \left(\frac{x'(\xi+\psi)}{\xi-z'}, \frac{y'(\xi+\psi)}{\xi-z'}, -\psi\right)$.

Finally, the composition $\pi_{\xi,\psi} = \pi_{\Omega_\psi} \circ \pi_{S^2}$, projects points of $(\mathbb{R}^3)^*$ onto the image plane Ω_ψ. Since π_{Ω_ψ} depends on the point $\mathbf{p}_\xi$, hence the domain of $\pi_{\xi,\psi}$ is the set $\mathcal{D}(\pi_{\xi,\psi}) = \{(x,y,z) \in (\mathbb{R}^3)^* : \frac{z}{\|\mathbf{p}\|} < \xi\}$. Thus, if $\mathbf{p} = (x,y,z) \in \mathcal{D}(\pi_{\xi,\psi})$, then

$$\begin{aligned}
\pi_{\xi,\psi}(\mathbf{p}) &= (\pi_{\Omega_\psi} \circ \pi_{S^2})(\mathbf{p}) \\
&= \pi_{\Omega_\psi}(\pi_{S^2}(\mathbf{p})) \\
&= \pi_{\Omega_\psi}\left(\frac{x}{\|\mathbf{p}\|}, \frac{y}{\|\mathbf{p}\|}, \frac{z}{\|\mathbf{p}\|}\right) \\
&= \left(\frac{\frac{x}{\|\mathbf{p}\|}(\xi+\psi)}{\xi - \frac{z}{\|\mathbf{p}\|}}, \frac{\frac{y}{\|\mathbf{p}\|}(\xi+\psi)}{\xi - \frac{z}{\|\mathbf{p}\|}}, -\psi\right) \\
&= \left(\frac{x(\xi+\psi)}{\xi\|\mathbf{p}\| - z}, \frac{y(\xi+\psi)}{\xi\|\mathbf{p}\| - z}, -\psi\right).
\end{aligned}$$

Thus, in the composition of the two projections we have coordinates: $\bar{x} = \frac{x(\xi+\psi)}{\xi\|p\|-z}, \bar{y} = \frac{y(\xi+\psi)}{\xi\|p\|-z}$ and $\bar{z} = -\psi$.

Observation 6.1.

(1) *The function $\pi_{\xi,\psi} : \mathcal{D}(\pi_{\xi,\psi}) \to \Omega_\psi$ is not bijective, since π_{S^2} and π_{Ω_ψ} are not injective (one-to-one) and surjective (onto) respectively.*

(2) *It is possible to obtain a bijective function from $\pi_{\xi,\psi}$, restricting the domain and codomain in the following way: Let $\Omega_{z_0} := \{(x,y,z_0) \in \mathbb{R}^3 : $ for a fixed $z_0\}$ and $\Omega_{lm} := \{\mathbf{q} \in \Omega_\psi : \mathbf{q} = \pi_{\xi,\psi}(\mathbf{p})$ for some $\mathbf{p} \in \Omega_{z_0}\}$. Thus $f : \Omega_{z_0} \to \Omega_{lm}$ defined by $f(\mathbf{p}) = \pi_{\xi,\psi}(p)$ is a bijection.*

The parameters to get the parabolic and hyperbolic projections given in Geyer and Daniilidis (2000) are:

	Parabolic	Hyperbolic
(ξ, ψ)	$(1, 2d_{fv} - 1)$	$\left(\frac{d}{\sqrt{d^2+4d_{fv}^2}}, \frac{d(1-2d_{fv})}{\sqrt{d^2+4d_{fv}^2}}\right)$

In both cases, d_{fv} is the distance from the focus of the mirror to its vertex. In the case of a hypercatadioptric camera, d determines the distance between the focus of the mirror and the optical center of the perspective (conventional) camera that gets the image. Fig. 8 shows the paraboloid and hyperboloid projection of the critical curves on the reduced space.

6.2. Problem statement

The differential drive robot (DDR) is equipped with an omnidirectional camera placed in the center of the disk shaped DDR surface, at height a (see Fig. 9). The distance to the optical center of the pinhole camera is measured from this location (center of the disk shaped robot surface).

We denote Ω_{RS} to the reduced space and we shall define $\pi : \Omega_{RS} \to \Omega_{lm}$ as in Observation 6.1. The set Ω_{lm} is called the **image space**. The objective is to define a feedback image-based motion strategy from Ω_{lm} via π such that it is **congruent** with a motion strategy based on the states over Ω_{RS} (Jacobo et al., 2015).

We will assume three local reference frames: $(\mathbf{XYZ})_0$, $(\mathbf{XYZ})_{cam}$, $(\mathbf{XYZ})_{RS}$ (see Fig. 9). The first one with origin at $\mathbf{O}_0$, the focus of the mirror of the omnidirectional camera. The origin of the second one $\mathbf{O}_{cam}$ is located in the camera's optical center. Finally, the third one with origin $\mathbf{O}_{RS}$ is located on the center of the surface of the disk shaped DDR. We assume that the three local reference frames are aligned, and that $(\mathbf{XYZ})_0$ and $(\mathbf{XYZ})_{RS}$ are translated over the axis $\mathbf{Z}_0$, $(\mathbf{XYZ})_{cam}$ with $z = -d$ and $(\mathbf{XYZ})_{RS}$ with $z = -(a+d)$. Let $z_0 = -(a+d)$, thus, the reduced space is the plane $\Omega_{RS} := (\mathbf{XY})_{RS} = \{(x,y,z) \in \mathbb{R}^3 : z = z_0\}$.

Note 1. Given that z_0 is fixed, if $\mathbf{p} \in \Omega_{RS}$ then we will write $\mathbf{p} = (x,y)$ instead of $\mathbf{p} = (x,y,z_0)$, but considering z_0 in the calculations.

6.3. A solution

For a pursuer equipped with an omnidirectional camera the projection of the (x,y) coordinates of the evader are available in the image. However, note that the critical curves delimiting the regions defining the pursuer's strategy are not observable in the

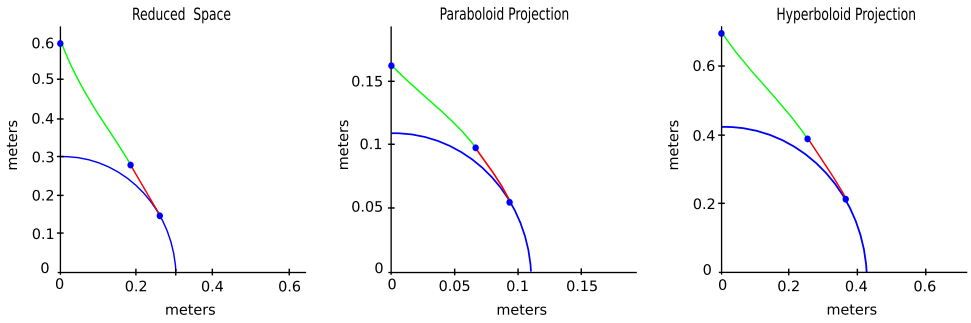

Fig. 8. Parabolic and Hyperbolic projections of the reduced space.

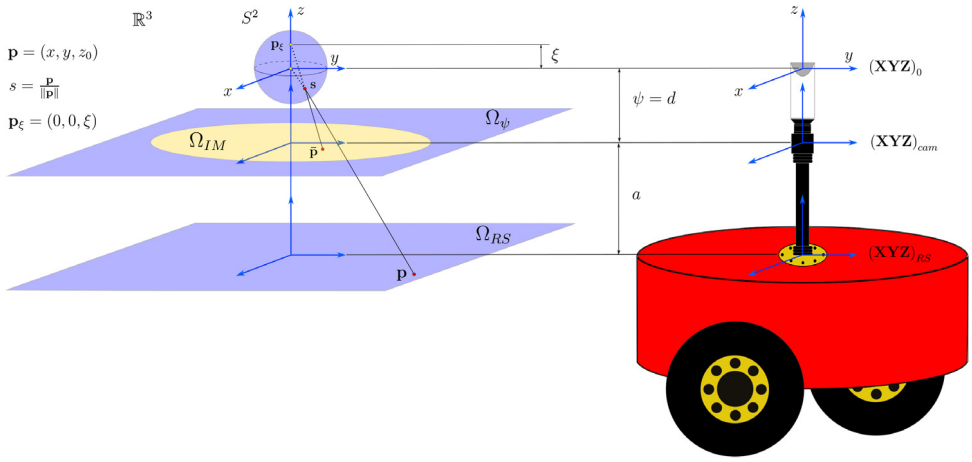

Fig. 9. Local reference frames and the DDR.

image. Furthermore, even if the curves delimiting regions would be observable, there is no guarantee that in the image, the perceived world, "distorted" due to the nonlinear projection of the omnidirectional camera, would preserve the state (x, y) within the correct "distorted" regions. In Theorem 3, we shall prove that the location of the evader on the image can be directly used by the pursuer to define its motion strategy. That is, the pursuer is able to apply its motion strategy using the image without explicitly reconstructing the evader position.

Let us start with the following proposition and recall that in the reduced space all the orientations are measured with respect to the positive y-axis. Thus, given a point $\mathbf{p} = (x, y) \in \Omega_{RS}$, its polar coordinates are defined by $\mathbf{p} = (r, \phi) = (\sqrt{x^2 + y^2}, \tan^{-1}(\frac{x}{y}))$.

The following proposition, establishes that the angular measure of the evader position is the same in both, on the reduced space and on the image space.

Proposition 3. *If $\bar{\mathbf{p}} = \pi(\mathbf{p}) \in \Omega_{Im}$, then the polar coordinates of $\bar{\mathbf{p}}$ are given by*

$$\bar{\mathbf{p}} = (\bar{r}, \bar{\phi}) = \left(\frac{r(\xi + \psi)}{\xi\sqrt{r^2 + z_0^2} - z_0}, \phi \right).$$

Proof. First we prove that $\bar{r} = \frac{r(\xi+\psi)}{\xi\sqrt{r^2+z_0^2}-z_0}$.

We have $\bar{\mathbf{p}} = (\bar{x}, \bar{y}) = \left(\frac{x(\xi+\psi)}{\xi\sqrt{x^2+y^2+z_0^2}-z_0}, \frac{y(\xi+\psi)}{\xi\sqrt{x^2+y^2+z_0^2}-z_0} \right) = \left(\frac{x(\xi+\psi)}{\xi\sqrt{r^2+z_0^2}-z_0}, \frac{y(\xi+\psi)}{\xi\sqrt{r^2+z_0^2}-z_0} \right)$.

Then

$$\bar{r} = \sqrt{\bar{x}^2 + \bar{y}^2} = \sqrt{\frac{x^2(\xi+\psi)^2}{(\xi\sqrt{r^2+z_0^2}-z_0)^2} + \frac{y^2(\xi+\psi)^2}{(\xi\sqrt{r^2+z_0^2}-z_0)^2}}$$
$$= \sqrt{\frac{(x^2+y^2)(\xi+\psi)^2}{(\xi\sqrt{r^2+z_0^2}-z_0)^2}} = \frac{\sqrt{x^2+y^2}\sqrt{(\xi+\psi)^2}}{\sqrt{\left(\xi\sqrt{r^2+z_0^2}-z_0\right)^2}}$$
$$= \frac{r|\xi+\psi|}{|\xi\sqrt{r^2+z_0^2}-z_0|}.$$

As $\xi \in [0, 1]$ and $\psi \geq 0$, then $|\xi + \psi| = \xi + \psi$.

On the other hand, $|\xi\sqrt{r^2+z_0^2} - z_0| = |\xi\sqrt{r^2+z_0^2} + (-z_0)|$. Since $z_0 = -(a + d)$ where a and d are positive numbers, thus $-z_0 > 0$. Then $\xi\sqrt{r^2+z_0^2} + (-z_0) > 0$. $|\xi\sqrt{r^2+z_0^2} + (-z_0)| = \xi\sqrt{r^2+z_0^2} + (-z_0) = \xi\sqrt{r^2+z_0^2} - z_0$. Hence

$$\frac{r\ |\xi+\psi|}{|\xi\sqrt{r^2+z_0^2}-z_0|} = \frac{r\ (\xi+\psi)}{\xi\sqrt{r^2+z_0^2}-z_0}.$$

Now we prove $\bar{\phi} = \phi$.

One has that $\tan(\bar{\phi}) = \frac{\bar{x}}{\bar{y}} = \frac{\frac{x(\xi+\psi)}{\xi\sqrt{r^2+z_0^2}-z_0}}{\frac{y(\xi+\psi)}{\xi\sqrt{r^2+z_0^2}-z_0}} = \frac{x}{y} = \tan(\phi)$.

Hence $\bar{\phi} = \phi$. ■

Now, we will prove that the function that defines the projection of the location of a point in the reduced space is strictly increasing with respect to r.

Lemma 3. *Let* $\mathbb{R}_{\geq 0} := \{x \in \mathbb{R} : x \geq 0\}$, $g : \mathbb{R}_{\geq 0} \to \mathbb{R}_{\geq 0}$ *be defined by* $g(r) = \frac{r(\xi+\psi)}{\xi\sqrt{r^2+z_0^2}-z_0}$. *Then* g *is strictly increasing.*

Proof. The derivative $\frac{d}{dr}g(r)$ is given by

$$\frac{d}{dr}g(r) = (\xi+\psi)\frac{\xi\sqrt{r^2+z_0^2} - z_0 - r^2\xi(r^2+z_0^2)^{-1/2}}{(\xi\sqrt{r^2+z_0^2}-z_0)^2}.$$

It is clear that $\frac{d}{dr}g(r) > 0$ if and only if

$$\xi\sqrt{r^2+z_0^2} - z_0 - r^2\xi(r^2+z_0^2)^{-1/2} > 0$$

namely, if and only if,

$$\frac{\left(\xi(r^2+z_0^2)^{1/2} - z_0\right)(r^2+z_0^2)^{1/2} - r^2\xi}{(r^2+z_0^2)^{1/2}} > 0$$

if and only if

$$(\xi(r^2+z_0^2)^{1/2} - z_0)(r^2+z_0^2)^{1/2} - r^2\xi > 0$$

if and only if

$$\xi z_0^2 - z_0(r^2+z_0^2)^{1/2} > 0.$$

Since $-z_0 > 0$ it follows that $-z_0(r^2+z_0^2)^{1/2} > 0$. Then $\xi z_0^2 - z_0(r^2+z_0^2)^{1/2} > 0$. Thus $\frac{dg}{dr}$ is strictly positive and hence, g is strictly increasing. ■

Proposition 4. *Let* $\mathbf{p}_1 = (r_1, \phi)$ *and* $\mathbf{p}_2 = (r_2, \phi)$ *be two points in* Ω_{RS}, *and* $\bar{\mathbf{p}}_1 = (\bar{r}_1, \phi)$, *and* $\bar{\mathbf{p}}_2 = (\bar{r}_2, \phi)$ *their respective projections on the image space. Then* $\bar{r}_1 < \bar{r}_2$, *if and only if,* $r_1 < r_2$.

Proof. By Proposition 3 we have that for any $\mathbf{p} = (r, \phi) \in \Omega_{RS}$, its projection is given by $\bar{\mathbf{p}} = (\bar{r}, \phi)$, where $\bar{r} = \frac{r(\xi+\psi)}{\xi\sqrt{r^2+z_0^2}-z_0}$. Let us note that $\bar{r} = g(r)$ where g is the function defined in Lemma 3. So, for $\mathbf{p}_1 = (r_1, \phi)$ and $\mathbf{p}_2 = (r_2, \phi)$ in Ω_{RS}, since g is strictly increasing, the conclusion follows. ■

It is important to note that in Proposition 4 both $\mathbf{p}_1$ and $\mathbf{p}_2$ lie on the same straight line in the reduced space passing through the origin $\mathbf{O}_{RS}$ since both points have the same coordinate ϕ. In the same way their respective projections are on the same straight line on the image space passing through the origin $\mathbf{O}_{Im}$.

Note 2. We now recall some concepts previously defined in Jacobo et al. (2015):

- For a given point $(r, \phi) \in BS$, Lemma 11 in Appendix tells us that $r = r_B$ where r_B is given in the same lemma. Let us note that the value of r_B depends on the value of ϕ.
- The angle of the frontier point between the transition surface and the barrier is denoted by ϕ_{TS}.
- The angle ϕ_B is equal to the angle S, which determines the usable part and the point where the barrier begins in retro-time.

Observation 6.2.

(1) *If* $F(r, \phi) = 0$ *denotes Eq. (A.2) in Lemma 10 in Appendix, and for each* $\phi \in (0, \phi_{TS})$ *we define* $F_\phi(r) = F(r, \phi)$, *then* $F_\phi(r) = 0$ *is a polynomial equation of degree four, where* ϕ_{TS} *is the orientation in the reduced space delimiting the transition surface TS and the barrier BS.*

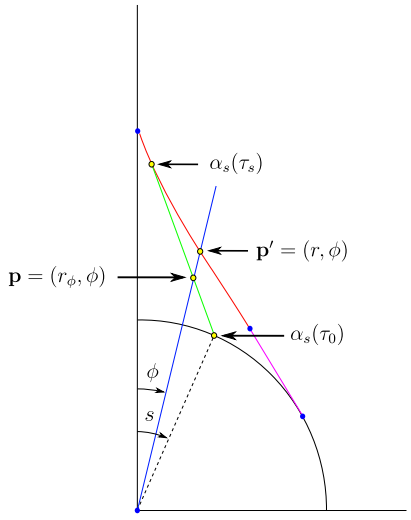

Fig. 10. The point $\mathbf{p} = (r_\phi, \phi)$ cannot be in the region RS.

(2) *If* R_ϕ *is the set of all positive roots of* $F_\phi(r) = 0$, *that is,* $R_\phi := \{r > 0 : F_\phi(r) = 0\}$, *then it is clear that:*

   (a) $R_\phi \neq \emptyset$ *by construction of the transition surface (see Ruiz et al., 2013 for details).*
   (b) R_ϕ *has at most four elements.*
   (c) *There exists a unique* $r_\phi \in R_\phi$ *such that* $(r_\phi, \phi) \in TS$.
   (d) *If* $r \in R_\phi$ *then* $r > l$ *where* l *is the robot's radius.*

For any angle $\phi \in (0, \phi_{TS})$, the following lemma tells us what is the radius r_ϕ such that the point (r_ϕ, ϕ) is on the transition surface. Besides, this radius is unique.

Lemma 4. *Let* $\phi \in (0, \phi_{TS})$, *then* $r_\phi := \mathbf{min}\{r : r \in R_\phi\}$ *is such that* $(r_\phi, \phi) \in TS$.

Proof. Recall that from Ruiz et al. (2013) for each angle $s \in (0, S)$ the retro-time straight line trajectories in the reduced space beginning on the UP are defined by

$$\begin{aligned} x(\tau) &= -\tau V_e^{max}\sin s + l\sin s \\ y(\tau) &= -\tau V_e^{max}\cos s + \tau V_p^{max} + l\cos s. \end{aligned} \tag{11}$$

Moreover, if $s \in [0, \tan^{-1}(\rho_v, \rho_d)]$ then the trajectory reaches the y-axis at $\tau_c = l/V_e^{max}$. If $s \in (\tan^{-1}(\rho_v, \rho_d), S)$ then the retro-time straight line trajectory ends at $\tau_s = \frac{b\cos s}{V_p^{max}\sin s}$.

Now let $\mathbf{p} = (r_\phi, \phi)$. If R_ϕ has a unique element then the result is clear. Let us assume that there exists $r \in R_\phi$, such that $r > r_\phi$ and $\mathbf{p}' := (r, \phi) \in TS$ (see Fig. 10). Then $\mathbf{p} \in R_S$. So, for some angle $s \in (0, S)$ the retro-time straight line trajectory $\alpha_s(\tau) := (x(\tau), y(\tau))$ defined by s contains the point $\mathbf{p}$, that is, $\mathbf{p} = \alpha_s(\tau_\mathbf{p})$ for some $\tau_\mathbf{p}$.

Since $\mathbf{p}$ is not an extreme point of α_s, we have two cases:

(1) If $s \in [0, \tan^{-1}(\rho_v, \rho_d)]$ then $\tau_\mathbf{p} < \tau_c$.
(2) If $s \in (\tan^{-1}(\rho_v, \rho_d), S)$ then $\tau_\mathbf{p} < \tau_s$.

In both cases we have $\tau_\mathbf{p} < \tau_s$.

On the other hand, equation $F(\rho, \phi) = 0$ in Lemma 10 of Appendix, was constructed in Jacobo et al. (2015). By this construction, the unique point of the trajectory α_s that satisfies equation $F(\rho, \phi) = 0$ is the final point of the trajectory given when $\tau = \tau_s$, that is, the point $\alpha_s(\tau_s)$. Thus $F(\mathbf{p}) = F(r_\phi, \phi) \neq 0$. Then $F_\phi(r_\phi) \neq 0$, which contradicts that $r_\phi \in R_\phi$. Therefore the conclusion follows. ■

The partition of the first quadrant of Ω_{RS} contains regions R_R and R_S (see Fig. 2(b)). These regions are equivalent classes defined by the controls. Thus, two points are related if and only if they have assigned the same control. In this way, all the points in region R_R have assigned the controls $(u_1, u_2) = (+V_p^{max}, -V_p^{max})$, while the points in region R_S have assigned the controls $(u_1, u_2) = (+V_p^{max}, +V_p^{max})$.

In the following theorem, we propose a feedback motion strategy based on the image space, that is congruent with the motion strategy obtained in Jacobo et al. (2015). The motion strategy below is for the first quadrant of the reduced space; there are analogous motion strategies for the other quadrants.

Theorem 3. *Let $\bar{\mathbf{p}} = (\bar{r}, \phi) \in \Omega_{Im}$. The optimal controls for the DDR in the first quadrant of Ω_{Im} are:*

$$\begin{matrix} u_1 = +V_p^{max} \\ u_2 = -V_p^{max} \end{matrix} \text{ if } \begin{cases} \phi \in (0, \phi_{TS}) & \text{and } \bar{r} \geq g(r_\phi) \\ \phi \in [\phi_{TS}, \phi_B] & \text{and } \bar{r} > g(r_B) \\ \phi \in (\phi_B, \frac{\pi}{2}] & \text{and } \bar{r} \geq g(l) \end{cases}$$

$$\begin{matrix} u_1 = +V_p^{max} \\ u_2 = +V_p^{max} \end{matrix} \text{ if } \begin{cases} \phi \in (0, \phi_{TS}) & \text{and } \bar{r} < g(r_\phi) \\ \phi \in [\phi_{TS}, \phi_B] & \text{and } \bar{r} < g(r_B) \end{cases}$$

where $g(r) = \frac{r(\xi+\psi)}{\xi\sqrt{r^2+z_0^2}-z_0}$ is the function in Lemma 3.

Proof. Let us start by observing that the strategy is well defined, that is, given a point $\bar{\mathbf{p}} \in \Omega_{Im}$, there exists a unique pair of controls $\mathbf{u} = (u_1, u_2)$ associated to $\bar{\mathbf{p}}$. Since $\pi : \Omega_{RS} \to \Omega_{Im}$ is a bijection, there exists a unique $\mathbf{p} = (r, \phi) \in \Omega_{RS}$ such that $\pi(\mathbf{p}) = \bar{\mathbf{p}}$.

Let us consider the different possible intervals of the values of ϕ. We have three possibilities:

(1) The interval $\phi \in (0, \phi_{TS})$ delimits the transition surface TS. By Lemma 4, There exists r_ϕ such that $(r_\phi, \phi) \in TS$.
   (a) If $\bar{r} \geq g(r_\phi)$ then by Proposition 4 we have $r \geq r_\phi$, which implies that $\mathbf{p} \in R_R$ if $\bar{r} > g(r_\phi)$ or $\mathbf{p} \in TS$ if $\bar{r} = g(r_\phi)$. Then the associated controls to $\bar{\mathbf{p}}$ are $u_1 = +V_p^{max}$ and $u_2 = -V_p^{max}$.
   (b) If $\bar{r} < g(r_\phi)$ then $r < r_\phi$, which implies $\mathbf{p} \in R_S$. Therefore the associated controls to $\bar{\mathbf{p}}$ are $u_1 = +V_p^{max}$ and $u_2 = +V_p^{max}$.

(2) The interval $[\phi_{TS}, \phi_B]$ delimits the barrier BS. By Lemma 11 in Appendix, there exists r_B such that $(r_B, \phi) \in TS$. Analogously to previous case, the associated controls to $\bar{\mathbf{p}}$ are
   (a) $u_1 = +V_p^{max}$ and $u_2 = -V_p^{max}$ if $\bar{r} > g(r_B)$.
   (b) $u_1 = +V_p^{max}$ and $u_2 = +V_p^{max}$ if $\bar{r} < g(r_B)$.

(3) In the interval $\phi \in (\phi_B, \frac{\pi}{2}]$, we only have the option $\bar{r} \geq g(l)$. Then $r \geq l$ and hence $\mathbf{p} \in R_R$. Therefore, the associated controls to $\bar{\mathbf{p}}$ are $u_1 = +V_p^{max}$ and $u_2 = -V_p^{max}$. ■

In Theorem 3, we have proved that the location of the evader on the image can be directly used by the pursuer to define its motion strategy. That is, the pursuer is able to apply its motion strategy using the image without reconstructing the evader's position. Thus, we have developed a fully image-based control law.

This method has the following advantages compared with the one given in Jacobo et al. (2015): It requires less computations and it does not need to observe seven points on the evader, which is required by the estimation based on the 1-D trifocal tensor, hence, it is more robust to occlusions and noise in the image.

6.4. A commutative diagram of the congruent motion strategies

The robot is equipped with an omnidirectional camera (which can be considered an instance of the abstract sensor in the context of LaValle, unpublished), such that $\pi : \Omega_{RS} \to \Omega_{Im}$, where Ω_{Im} is the observation in the image space and Ω_{RS} the reduced space. Let U be the control space, let $\pi_{RS} : \Omega_{RS} \to U$, and $\pi_{Im} : \Omega_{Im} \to U$ be the robot motion strategies with feedback based on Ω_{RS} and Ω_{Im} respectively.

In this work, we have shown that the proposed feedback motion strategy based on the image space is congruent with the feedback motion strategy obtained in Jacobo et al. (2015) based on the state space, yielding the following commutative diagram.

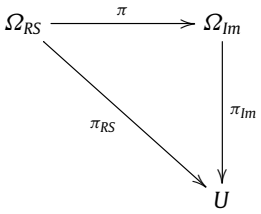

7. Conclusions and future work

In this paper, we have analyzed a pursuit-evasion game in which the set of admissible controls of the evader varies with time. From the Nash property it follows that if the evader deviates from its maximum potential speed, then the capture time shall not increase for a pursuer that follows a motion strategy generated based on the maximum potential evader's speed. However, in our first result, we have proposed another strategy for the pursuer that for certain scenarios, further reduces the capture time compared with the strategy in Nash Equilibrium (based on the maximum potential evader's speed). In our second result, we have shown that, under non-anticipative strategies, a pursuer strategy that uses the instantaneous evader speed, *does not always guarantee* to improve the payoff for the pursuer, nor the capture of the evader. Hence, we concluded that the evader's location is the relevant information for the pursuer to know. Finally, in our third result we have shown that the location of the evader on the image can be directly used by the pursuer to define its motion strategy, in spite of the distortion of the state space suffered on the image. That is, the pursuer is able to apply its motion strategy using the image without explicitly reconstructing the evader's position.

In an actual implementation of the pursuer control law, sensor errors can produce chattering (Zelikin & Borisov, 2012) in the transitions between regions, we believe that a hysteresis filtering on the sensor reading might alleviate the issue, however, this issue is out of the scope of the paper and we propose as future work to analyze it in detail. Also as future work, we will include acceleration bounds in the solution of this problem. Finally, we would like to analyze under what settings *anticipative strategies* (Friedman, 2006) do improve the pursuer's payoff when the players' control sets vary with time.

Appendix. Previous supporting results

In this appendix, we present some lemmas and theorems which are used in this work. Theorem 4 and Lemmas 5–9 were obtained in Ruiz et al. (2013) and Lemmas 10, 11 and Theorem 5 were obtained in Jacobo et al. (2015). For the proofs of these theorems and lemmas please see Jacobo et al. (2015) and Ruiz et al. (2013).

The retro-time is denoted $\tau = t_f - t$, in which t_f is the termination time of the game and t the current time.

Theorem 4. *If $\rho_v < |\tan S|/\rho_d$ the DDR can capture the evader from any initial configuration in the playing space. Otherwise the barrier separates the playing space into two regions, one of them contiguous to the UP. The DDR can only force the capture in the region contiguous to UP, in which case, the DDR follows a straight line in the realistic space when it captures the evader.*

Lemma 5. *The trajectories in Eq. (A.1) that reach the y-axis in the first quadrant, reach it at $y = l/\rho_v$.*

$$\begin{aligned} x(\tau) &= -\tau V_e^{\max} \sin s + l \sin s \\ y(\tau) &= \tau(-V_e^{\max} \cos s \pm V_p^{\max}) + l \cos s. \end{aligned} \tag{A.1}$$

Lemma 6. *The DDR switches controls and it starts a rotation in place in the realistic space, at $\tau_s = |\frac{b \cos s}{V_p^{\max} \sin s}|$. If $s \in [0, \pi]$, u_2^* switches first, otherwise u_1^* does.*

Lemma 7. *The barrier consists of a straight line segment, and it intersects the y -axis in the first quadrant if $\rho_v \geq |\tan S|/\rho_d$ where $S = \cos^{-1}(\rho_v)$ is the angle at the BUP.*

This lemma implies that for $S = \cos^{-1}(V_e/V_p)$ then $\tau = (b \cos S)/(V_p \sin S)$.

Lemma 8. *The retro-time trajectories reaching the y-axis in the first quadrant have an orientation $s \in [0, \tan^{-1}(\rho_v \rho_d)]$ at the UP.*

Lemma 9. *The straight lines trajectories that have an orientation $s \in (\tan^{-1}(\rho_v \rho_d), \cos^{-1}(\rho_v)]$ in the UP of the first quadrant terminate when the DDR switches controls.*

Lemma 10. *If the right term in the following equation is larger than 0, then the state is above the transition surface, that is, it is in region R_R.*

$$\begin{aligned} 0 \;=\; & r^4 \sin^2(\phi)\cos^2(\phi) + r^4 \sin^4(\phi) + 2br^3 \sin^3(\phi) \\ & + b^2 r^2 \sin^2(\phi) - \rho_v^2 b^2 r^2 \cos^2(\phi) + 2\rho_v blr^2 \sin(\phi)\cos(\phi) \\ & + 2\rho_v b^2 lr \cos(\phi) - l^2 r^2 \sin^2(\phi) - 2bl^2 r \sin(\phi) - l^2 b^2. \end{aligned} \tag{A.2}$$

Lemma 11. *If $(r, \phi) \in BS$ then*

$$r = r_B = \frac{V_p^{max} l \sin(S)}{V_p^{max} \sin(\phi) - V_e^{max} \sin(\phi - S)}. \tag{A.3}$$

Theorem 5. *The optimal controls for the pursuer are*

(1) $u_1 = +V_p^{max}, u_2 = -V_p^{max}$ *if* $(r, \phi) \in R_R$, *or equivalent:*

- (a) $\phi \in (0, \phi_{TS})$ *and Equation in Lemma 10* ≥ 0 *or*
- (b) $\phi \in [\phi_{TS}, \phi_B]$ *and* $r > r_B$ *or*
- (c) $\phi \in (\phi_B, \frac{\pi}{2}]$ *and* $r \geq l$.

In the other case, the optimal controls are

(2) $u_1 = +V_p^{max}, u_2 = +V_p^{max}$ *if:*

- (a) $\phi \in (0, \phi_{TS})$ *and Equation in Lemma 10* < 0 *or*
- (b) $\phi \in [\phi_{TS}, \phi_B]$ *and* $r < r_B$.

References

Balkcom, D. J., & Mason, M. T. (2002). Time optimal trajectories for bounded velocity differential drive vehicles. *International Journal of Robotics Research*, *21*(3), 219–232.

Bandyopadhyay, T., Ang Jr., M. H., & Hsu, D. (2007). Motion planning for 3-D target tracking among obstacles. In *Int. symp. on robotics research* (pp. 267–279).

Başar, T., & Olsder, G. (1999). Dynamic noncooperative game theory, 2nd ed. SIAM series in classics in applied mathematics, Philadelphia.

Becerra, I., Macias, V., & Murrieta-Cid, R. (2015). On the value of information in a differential pursuit-evasion game. In *Proc. IEEE international conference on robotics and automation*, Seattle, Washington (pp. 4768–4774).

Bhattacharya, S., & Hutchinson, S. (2010). On the existence of nash equilibrium for a two player pursuit-evasion game with visibility constraints. *International Journal of Robotics Research*, *29*(7), 831–839.

Bhattacharya, S., & Hutchinson, S. (2011). A cell decomposition approach to visibility-based pursuit evasion among obstacles. *International Journal of Robotics Research*, *30*(14), 1709–1727.

Chaumette, F., & Hutchinson, S. (2006). Visual servo control. I. Basic approaches. *IEEE Robotics and Automation Magazine*, *13*(4), 82–90.

Chung, T., Hollinger, G., & Isler, V. (2011). Search and pursuit-evasion in mobile robotics: A survey. *Autonomous Robots*, *31*(4), 299–316.

Elliott, R. J., & Kalton, N. J. (1972). *The existence of value in differential games, Vol. 126*. American Mathematical Soc..

Flynn, J. (1974). Lion and man: The general case. *SIAM Journal on Control*, *12*, 581–597.

Friedman, A. (2006). *Differential games*. Dover Ed edition.

Geyer, C., & Daniilidis, K. (2000). A unifying theory for central panoramic systems and practical implications. In *Proceedings of European conference on computer vision*, Dublin (pp. 445–461).

Guibas, L., Latombe, J.-C., LaValle, S. M., Lin, D., & Motwani, R. (1999). Visibility-based pursuit-evasion in a polygonal environment. *International Journal of Computational Geometry & Applications*, *9*(5), 471–494.

Hollinger, G., Singh, S., Djugash, J., & Kehagias, A. (2009). Efficient multi-robot search for a moving target. *International Journal of Robotics Research*, *28*(2), 201–219.

Isaacs, R. (1965). *Differential games: A mathematical theory with applications to warfare and pursuit, control and optimization*. New York: John Wiley and Sons, Inc..

Isler, V., & Karnad, N. (2008). The role of information in the Cop-Robber game. *Theoretical Computer Science*, *3*(399), 179–190.

Jacobo, D., Ruiz, U., Murrieta-Cid, R., Becerra, H. M., & Marroquin, J. L. (2015). A visual feedback-based time-optimal motion policy for capturing an unpredictable evader. *International Journal of Control*, *88*(4), 663–681.

Jung, B., & Sukhatme, G. (2002). Tracking targets using multiple robots: the effect of environment occlusion. *Auton Robot*, *12*, 191–205.

Karnad, N., & Isler, V. (2009). Lion and man game in the presence of a circular obstacle. In *Proc. IEEE int. conf. on intelligent robots and systems*.

LaValle, S. M. Sensor Lattices: A Preimage-Based Approach to Comparing Sensors, Unpublished work.

LaValle, S. M., González-Baños, H. H., Becker, C., & Latombe, J.-C. (1997). Motion strategies for maintaining visibility of a moving target. In *Proc. IEEE int. conf. robot. autom, Vol. 1* (pp. 731–736).

Lopez-Nicolas, G., Gans, N. R., Bhattacharya, S., Sagues, C., & Hutchinson, S. (2010). Homography-based control scheme for mobile robots with nonholonomic and field-of-view constraints. *IEEE Transactions on Systems, Man, and Cybernetics, Part B*, *40*(4), 1115–1127.

Merz, A. W. (1971). *The homicidal chauffeur–a differential game*. (Ph.D. Thesis), Stanford University.

Murrieta-Cid, R., Muppirala, T., Sarmiento, A., Bhattacharya, S., & Hutchinson, S. (2007). Surveillance strategies for a pursuer with finite sensor range. *International Journal of Robotics Research*, *26*(3), 233–253.

Murrieta-Cid, R., Ruiz, U., Marroquin, J. L., Laumond, J. P., & Hutchinson, S. (2011). Tracking an omnidirectional evader with a differential drive robot. *Auton Robot*, *31*(4), 345–366. Special Issue on Search and Pursuit/Evasion.

O'Kane, J. M. (2008). On the value of ignorance: Balancing tracking and privacy using a two-bit sensor. In *Proc. int. workshop algorithmic found. rob* (pp. 235–249).

Pontryagin, L. S., Boltyanskii, V. G., Gamkrelidze, R. V., & Mishchenko, E. F. (1962). *The mathematical theory of optimal processes*. JohnWiley.

Ruiz, U., Murrieta-Cid, R., & Marroquin, J. L. (2013). Time-optimal motion strategies for capturing an omnidirectional evader using a differential drive robot. *IEEE Transactions on Robotics*, *29*(5), 1180–1196.

Soueres, P., & Laumond, J. P. (1996). Shortest paths synthesis for a car-like robot. *IEEE Transactions on Automatic Control*, *41*(5), 672–688.

Tovar, B., & LaValle, S. M. (2008). Visibility-based pursuit - evasion with bounded speed. *International Journal of Robotics Research*, *27*(11–12), 1350–1360.

Vidal, R., Shakernia, O., Jin, H., Hyunchul, D., & Sastry, S. (2002). Probabilistic pursuit-evasion games: Theory, implementation, and experimental evaluation. *IEEE Transactions on Robotics and Automation*, *18*(5), 662–669.

Wang, H., Chen, Y., & Soueres, P. (2009). A geometric algorithm to compute time-optimal trajectories for a bidirectional steered robot. *IEEE Transactions on Robotics*, *25*(2), 399–413.

Zelikin, M. I., & Borisov, V. F. (2012). *Theory of chattering control: With applications to astronautics, robotics, economics, and engineering*. Springer Science & Business Media.

Vladimir Macias received his B.S. degree in Mathematics from Universidad de Guadalajara, Mexico, in 2005. He received his M.S. degree in Pure Mathematics from Centro de Investigación en Matemáticas (CIMAT), Guanajuato, Mexico, in 2011. He is currently (2017) pursuing a Ph.D. degree in Computer Science at CIMAT. He is mainly interested in motion planning, pursuit-evasion games and control theory.

Israel Becerra received the B.S. degree in Mechatronics Engineering from the Monterrey Institute of Technology and Higher Education, CEM (2007). He received the M.Sc. degree (2010) and Ph.D. degree (2015) both in Computer Science from CIMAT-Centro de Investigación en Matemáticas-, Guanajuato, Mexico. He is mainly interested in motion planning, pursuit-evasion games and probabilistic robotics. He is currently a postdoctoral researcher at University of Illinois working with professor Steven M. LaValle.

Rafael Murrieta-Cid received the B.S. degree in physics engineering from the Monterrey Institute of Technology and Higher Education, Monterrey, Mexico, in 1990 and the Ph.D. degree from the Institut National Polytechnique, Toulouse, France, in 1998. His Ph.D. research was done with the Robotics Group (RIA) of the LAAS-CNRS. In 1998–1999, he was a Postdoctoral Researcher with the Department of Computer Science, Stanford University, Stanford CA, USA. During 2002–2004, he was a Postdoctoral Researcher with the Beckman Institute and the Department of Electrical and Computer Engineering, University of Illinois at Urbana-Champaign (UIUC), Urbana, IL, USA. Since 2006, he has been a senior research scientist in the Centro de Investigación en Matemáticas, CIMAT, Guanajuato, México, and he is member of the Mexican National System of Researchers at level 2. In 2016, he was on a sabbatical leave at UIUC. His research interests include robotics, robot motion planning and control theory.

Hector M. Becerra received a degree in Electronics Engineering from the Tecnolgico Nacional de Mexico, campus Ciudad Guzmán, a M.Sc. a degree in Automatic Control from CINVESTAV-Guadalajara, Mexico, and a Ph.D. degree in Systems Engineering and Computer Science from the University of Zaragoza, Spain, in 2003, 2005 and 2011, respectively. He is currently a full researcher at Centro de Investigación en Matemáticas, CIMAT-Guanajuato, Mexico. His research interests include applications of automatic control to robotics, particularly the use of computer vision as main sensory modality.

Seth Hutchinson received his Ph.D. from Purdue University in 1988. In 1990 he joined the faculty at the University of Illinois in Urbana-Champaign, where he is currently a Professor in the Department of Electrical and Computer Engineering, the Coordinated Science Laboratory, and the Beckman Institute for Advanced Science and Technology. He served as Associate Department Head of ECE from 2001 to 2007. He currently serves on the editorial board of the International Journal of Robotics Research, and chairs the steering committee of the IEEE Robotics and Automation Letters. He was Founding Editor-in-Chief of the IEEE Robotics and Automation Society's Conference Editorial Board (2006–2008), and Editor-in-Chief of the IEEE Transaction on Robotics (2008–2013). He has published more than 200 papers on the topics of robotics and computer vision, and is coauthor of the books "Principles of Robot Motion: Theory, Algorithms, and Implementations", published by MIT Press, and "Robot Modeling and Control", published by Wiley. Hutchinson is a Fellow of the IEEE.